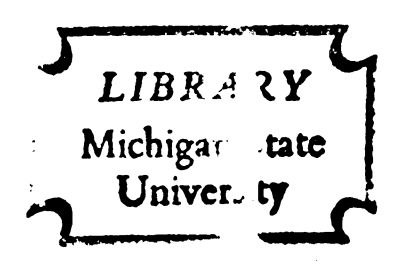
STUDIES OF TRANS-VINYLCYCLOPROPANE, METHYLDIFLUOROPHOSPHINE, AND METHOXYDIFLUOROPHOSPHINE BY MOLECULAR ROTATIONAL SPECTROSCOPY

Thesis for the Degree of Ph.D. MICHIGAN STATE UNIVERSITY EDWARD GEORGE CODDING 1971



This is to certify that the

thesis entitled

Studies of Trans-Vinylcyclopropane,
Methyldifluorophosphine, and Methoxydifluorophosphine
by Molecular Rotational Spectroscopy

presented by

Edward George Codding

has been accepted towards fulfillment of the requirements for

Ph.D. degree in Chemistry

Major professor

Date June 10, 1971

O-7639

ABSTRACT

STUDIES OF TRANS-VINYLCYCLOPROPANE, METHYLDIFLUOROPHOSPHINE,

AND METHOXYDIFLUOROPHOSPHINE BY MOLECULAR ROTATIONAL SPECTROSCOPY

Ву

Edward George Codding

A brief historical review of rotational spectroscopy is presented. The theory of rotational spectra, the coupling of internal rotation to the overall angular momentum of the molecule, the Stark effect, and molecular structure determination are discussed. A short description of the microwave spectrometer, including a description of a new binary decoder which is useful for placing accurate frequency markers on a spectral recording, is given.

The molecular rotational spectrum of trans-vinylcyclopropane in the ground and first three excited torsional states was analyzed. The B and C rotational constants were determined for all species by analysis of the spectral frequencies while the A rotational constant was estimated by analysis of an anomalous Stark effect of the 2_{02} - 3_{03} transition. The molecular dipole moments were determined to be μ_a = 0.486±0.007 D, μ_b = 0.0 D, μ_c = 0.110±0.003 D, μ_T = 0.498±0.007 D. An exhaustive search failed to disclose transitions assignable to another molecular configuration.

The molecular rotational spectrum of methyldifluorophosphine in the ground and first excited torsional state was analyzed. The three

rotational conditional conditional conditional condition of the height was det which was obtained assumptions are bond length, to the three rotational transfer here.

The three rotational tractional tractional tractional tractional tractions to be 422 call molecular concis to the fl

are r(PF) = 1

<(FPF) = 95.3

<(OCH₇) = 110

away from the

rotational constants were determined for both species. The molecular dipole moments were obtained as: μ_a = 2.047±0.002 D, μ_b = 0.0 D, μ_c = 0.194±0.03 D, μ_T = 2.056±0.03 D. The barrier to internal rotation of the methyl group was found to be 6.1 kcal/mole. The barrier height was determined from the torsional excitation energy, 325 cm $^{-1}$, which was obtained from relative intensity measurements in the microwave spectrum and direct observation in the infrared spectrum. If reasonable assumptions are made about the structure of the methyl group and the PF bond length, the PC bond length is determined to be 1.82 Å.

The molecular rotational spectra of the species, CH_3OPF_2 , $^{13}CH_3OPF_2$, $CH_3^{18}OPF_2$, and CD_3OPF_2 were investigated in the region 26.5-40. GHz. The three rotational constants were determined for all species. The rotational transitions are split by tunneling of the methyl group through the barrier hindering internal rotation. The barrier height was determined to be 422 cal/mole by analysis of these splittings. The structure of the molecular configuration having a plane of symmetry with the methyl group cis to the fluorines has been obtained. The bond lengths and bond angles are r(PF) = 1.586 Å, r(PO) = 1.572 Å, r(OC) = 1.446 Å, r(CH) = 1.09 Å, $(FPF) = 95.3^{\circ}$, $(FPO) = 101.5^{\circ}$, $(POC) = 123.5^{\circ}$, $(OCH_6) = 107.1^{\circ}$, $(OCH_7) = 110.7^{\circ}$, and $(HCH) = 109.4^{\circ}$. The methyl group is tilted 2.4° away from the fluorines relative to the OC bond.

STUDIES OF TRANS-VINYLCYCLOPROPANE, METHYLDIFLUOROPHOSPHINE, AND METHOXYDIFLUOROPHOSPHINE BY MOLECULAR ROTATIONAL SPECTROSCOPY

Ву

Edward George Codding

A THESIS

Submitted to
Michigan State University
in partial fulfillment of the requirements
for the degree of

DOCTOR OF PHILOSOPHY

Department of Chemistry

To my mother and father for their encouragement and faith through good times and bad, and to Penny for her ever present smile.

ACKNOWLEDGMENTS

I wish to extend my deepest gratitude to Professor Richard H.

Schwendeman for his guidance and encouragement throughout this investigation and the preparation of this thesis.

Financial support from the National Science Foundation, the Dow Chemical Company, and the Phillips Petroleum Company is gratefully acknowledged.

TABLE OF CONTENTS

I.	HISTORICAL BACKGROUND	1
II.	THEORY	4
	2.1 Introduction	12
III.	EXPERIMENTAL	18
	3.1 Introduction	20 20 21
IV.	MOLECULAR ROTATIONAL RESONANCE SPECTRUM OF TRANS- VINYLCYCLOPROPANE	23
	4.1 Introduction 4.2 Rotational Constants 4.3 Dipole Moment 4.4 The Anomalous Stark Effect of the M = 1 Component of the 2 ₀₂ -3 ₀₃ Transition 4.5 Discussion of Results	39
٧.	MOLECULAR ROTATIONAL RESONANCE SPECTRUM OF METHYLDIFLUOROPHOSPHINE	43
	5.1 Introduction 5.2 Rotational Constants 5.3 Molecular Structure 5.4 Barrier to Internal Rotation 5.5 Dipole Moment of Methyldifluorophosphine 5.6 The Anomalous Stark Effect of the M = 1 Component of the 1 ₀₁ -2 ₀₂ Transition 5.7 Discussion of Results	53 57 57
VI.	MOLECULAR ROTATIONAL RESONANCE SPECTRUM OF METHOXYDIFLUOROPHOSPHINE	
	6.1 Introduction	63 65 66

		Molecular Discussion																			
LIST OF	REFE	RENCES	 		•	•	•	•	•	•	•	•	•	•	•	•	•	•	•	•	85
APPENDI	х		 																		8 9

LIST OF TABLES

Table	e	Pag
1.	Notation for the Internal Rotation Problem	. 9
2.	Assumed Molecular Parameters for Trans-Vinylcyclopropane	. 25
3.	The Atomic Coordinates and Rotational Constants of Trans- Vinylcyclopropane in the Principal Axis System Using the Assumed Parameters of Table 2	. 26
4.	Comparison of Observed and Calculated Frequencies for the Ground and First Three Excited Torsional States of Trans-Vinylcyclopropane	. 30
5.	Rotational Constants and Principal Moments of Inertia for the Ground and First Three Excited Torsional States of Trans-Vinylcyclopropane	. 32
6.	Comparison of Observed and Calculated Frequencies for a ¹³ C Species of Trans-Vinylcyclopropane	. 36
7.	Rotational Constants and Principal Moments of Inertia for the ¹³ C Species of Trans-Vinylcyclopropane	. 36
8.	The Stark Effect and Dipole Moment of Trans-Vinylcyclopropane	.37
9.	Comparison of Dipole Moments of Some Related Hydrocarbons	. 38
10.	Assumed Molecular Parameters for Methyldifluorophosphine	. 45
11.	Atomic Coordinates and Rotational Constants of Methyldifluoro-phosphine in the Principal Axis System	.45
12.	Comparison of Observed and Calculated Frequencies for the Ground and First Excited Torsional State of Methyldifluorophosphine	.49
13.	Rotational Constants, Principal and Second Moments of Inertia for the Ground and First Excited Torsional States of Methyldifluorophosphine	.50
14.	The PC Bond Length, FPF and FPC Bond Angles as a Function of the PF Bond Length in Methyldifluorophosphine	.54

15.	Molecular Parameters for Some Difluorophosphine Derivatives54 $$
16.	The Stark Effect and Dipole Moment of Methyldifluorophosphine58
17.	Comparison of the Dipole Moments for Some Phosphine and Difluorophosphine Derivatives
18.	Barriers to Internal Rotation About the C-O Bond
19.	Comparison of Observed and Calculated Frequencies and Internal Rotation Splittings for ${\rm CH_3OPF_2}$ and ${\rm C^{13}H_3OPF_2}$
20.	Comparison of Observed and Calculated Frequencies and Internal Rotation Splittings for ${\rm CH_3OPF_2}$ and ${\rm CH_3O^{18}PF_2}$
21.	A-Level Rotational Constants, Principal and Second Moments of Inertia for the Normal and Three Isotopic Species of Methoxydifluorophosphine
22.	Internal Rotation Parameters for the Normal and Three Isotopic Species of Methoxydifluorophosphine
23.	Effective Rotational Constants, Principal and Second Moments of Inertia for the Normal and Three Isotopic Species of Methoxydifluorophosphine
24.	Principal Axis Coordinates for Methoxydifluorophosphine
25.	Calculated Bond Lengths and Bond Angles for Methoxydifluoro-phosphine
26.	Comparison of Results of Structural Studies on Some Phosphorous(V) Compounds
27.	Binary Representation of the Decimal Numbers Zero to Nine90

LIST OF FIGURES

Figur	e	Page
I.	Block diagram of a typical MRR spectrometer	19
II.	The projection of trans-vinylcyclopropane on to the molecular symmetry plane	27
III.	Plots of differences between rotational constants of trans-vinylcyclopropane in the vth torsional state and the ground vibrational state as a function of v	34
IV.	Projection of methyldifluorophosphine on to the molecular symmetry plane	46
٧.	Plots of 1/2(A-C) \underline{vs} . κ for the a) 6_{43} - 6_{42} , b) 7_{53} - 7_{52} , c) 8_{63} - 8_{62} and d) 9_{73} - 9_{72} Q-branch transitions of methyldifluorophosphine	48
VI.	Plots of 1/2(A-C) \underline{vs} . κ for a) 7_{53} - 7_{52} , b) 8_{63} - 8_{62} and c) 9_{73} - 9_{72} of the first excited torsional state of methyldifluorophosphine	52
VII.	Comparison of the observed and calculated Stark effect for the $ M =1$ component of the l_{01} - l_{02} transition	61
VIII.	Projection of methoxydifluorophosphine on to the molecular plane of symmetry	81
IX.	Symbols and truth tables for (a) NAND gates, (b) AND gates and (c) OR gates	91
χ.	Block diagram of the logic section of the binary decoder	93

I. HISTORICAL BACKGROUND

Although the first experiments in the microwave region were carried out as early as 1933 by Cleeton and Williams (1), active experimentation did not begin until after the development of 1.25 centimeter radar equipment during World War II. Much of the early work was devoted to the development of more sensitive experimental techniques and generally to theoretical and experimental studies of ammonia which was particularly suitable because of its very intense spectrum. That high resolution was attainable in the microwave region was demonstrated by the early work of Bleaney and Penrose (2,3) and Coles and Good (4) on the inversion spectrum of ammonia.

Hughes and Wilson (5) suggested that the absorption signal could be modulated by the application of a periodic electric Stark field to the sample. The tremendous increase in sensitivity due to this technique has made Stark modulated spectrometers the most important instruments in the microwave region.

Theory predicted that the Stark effect shift and splitting for linear molecules should be proportional to the square of the applied electric field strength and to the square of the dipole moment. Stark effect measurements carried out by Dakin, Good, and Coles (6) on carbonyl sulfide, OCS, confirmed the theory. The theory of the Stark effect was extended to asymmetric-top molecules by Golden and Wilson (7) and now dipole moments are routinely determined for many molecules by microwave

spectroscopy or molecular rotational resonance (MRR), as it has recently been called.

The high resolution available with MRR makes it possible to observe and study the hyperfine structure arising from internal rotations within the molecule. The theoretical problem of internal rotation was first considered by Nielsen (8) and Koehler and Dennison (9), and later by Kilb, Lin, and Wilson (10). Herschbach (11) has presented an extensive treatment of the internal rotation problem and has tabulated perturbation coefficients which are extremely useful in calculating the potential barrier to internal rotation. In addition, Wilson (12) has reviewed the subject of internal rotation discussing both the experimental methods available for obtaining values of the barrier height and the theoretical interpretations of the data. Analysis of the hyperfine structure resulting from internal rotation by the MRR technique is currently the most accurate method for determining low barriers.

The determination of molecular structures is probably the most important application of the MRR technique. The rotational constants which are obtained from the assignment of the spectrum are essentially reciprocal functions of the moments of inertia which are determined by the physical locations and masses of the atoms within the molecule. Internuclear distances and bond angles were first determined by varying these parameters until the computed moments of inertia reproduced the experimental moments of inertia of several isotopic species. A better method was suggested by Kraitchman (13) which provides for fitting the differences in the moments of inertia of two isotopically different molecules to determine the atomic coordinates of the substituted atom. This method requires substitution of all the nonequivalent atoms in the molecule and is insensitive to atoms which are located near a principal axis or

the molecular center of mass. Costain (14) has pointed out that structures obtained by the use of Kraitchman's relations are more reliable than those obtained by the direct fitting of the moments of inertia.

Because of vibration-rotation interactions it is difficult to relate the spectroscopically determined structure to the equilibrium or average molecular structure (15). However Herschbach and Laurie (16) have suggested a method for obtaining a good approximation of the average structure from the effective moments of inertia.

This thesis is concerned with the determination of the dipole moments, barriers to internal rotation, and structure parameters of the molecules vinylcyclopropane, methyldifluorophosphine, and methoxydifluorophosphine. The reasons for selecting these molecules and the results of the studies are described in Chapters IV, V and VI. Chapters II and III are concerned with the theory and practice of rotational spectroscopy.

Ì
\
1
1
1

II. THEORY

2.1 Introduction

In the calculation of molecular rotational energy levels, as with most quantum mechanical calculations, one attempts to make approximations which facilitate the calculations without adversely affecting the accuracy of the results. The primary assumption made is that the molecule may be treated as a rigid aggregate of point masses. This approximation may be justified theoretically, but there is also abundant empirical evidence that the transition frequencies calculated in this manner reproduce observed values to within the desired tolerances for all but the lightest molecules.

2.2 Rigid Rotor Model

If x_i , y_i and z_i are the effective rigid rotor coordinates of the i^{th} atom, then the moments of inertia and the products of inertia are respectively (17),

$$I_{xx} = \sum_{i=1}^{N} (y_i^2 + z_i^2)$$

$$I_{xy} = -\sum_{i=1}^{N} x_i y_i$$
(2-1)

where the sum is over all the atoms of molecules, the m_i are the atomic masses and x, y and z are cyclically permuted to obtain the remaining equations. If the origin of the coordinate system is located at the center of mass of the molecule, defined by,

$$\sum_{i}^{N} \overline{R}_{i} = 0$$

where \overline{R}_i is the position vector for the ith atom, the coordinate system may be rotated such that the products of inertia vanish and the inertial tensor becomes diagonal. The resulting diagonal elements are labeled I_a , I_b and I_c in order of increasing magnitude and are called the principal moments of inertia. The resulting coordinate axes are the principal axes and are labeled a, b and c to correspond to I_a , I_b and I_c respectively.

The rigid-rotor Hamiltonian may be written as (18),

$$H = \frac{4\pi^2}{h} (AP_a^2 + BP_b^2 + CP_c^2)$$
 (2-2)

where $A = \frac{h}{8\pi^2 I_a}$, $B = \frac{h}{8\pi^2 I_b}$ and $C = \frac{h}{8\pi^2 I_c}$, $(A \ge B \ge C)$ and the P_i 's are the principal axis components of the rotational angular momentum.

Solutions of the Schrödinger Equation, $H\psi = E\psi$, cannot be given in closed form if all three rotational constants are different. However, when two of the constants are equal, which is the symmetric rotor case, solutions are readily obtained. The eigenfunctions of the symmetric rotor case may be used as basis functions for construction of a Hamiltonian matrix for an asymmetric rotor ($A\neq B\neq C$). Diagonalization of the Hamiltonian yields the energies for the asymmetric rotor.

By using the commutation relations for angular momenta in a moleculefixed axis system (19),

$$[Px,Py] = -i\hbar Pz$$

 $[Py,Pz] = -i\hbar Px$ (2-3)
 $[Pz,Px] = -i\hbar Py$

the matrix elements of the squares of the angular momenta may be evaluated in a basis set in which P^2 and P_z are diagonal (20,21),

In these expressions $J = 0, 1, 2 \dots$ etc. and $K = 0, \pm 1, \pm 2 \dots$, $\pm J$ represent the quantum numbers for the total angular momentum and the projection of the total angular momentum on the molecule figure axis respectively. The combination of J and K uniquely label the energy levels.

For a prolate symmetric top, for which A>B=C, the matrix of the Hamiltonian of Eq. 2-2 may be shown to be diagonal. The diagonal values are the prolate symmetric top energy levels which may be written as (22),

$$E = h[BJ(J+1) + (A-B)K^{2}]$$
 (2-5)

For an oblate symmetric top for which A = B>C

$$E = h[AJ(J+1) + (C-A)K^{2}]$$
 (2-6)

For an asymmetric rotor J is still a good quantum number since the total angular momentum is a constant of the motion. However, K is not a good quantum number since there is no longer a molecular axis along which the projection of J is a constant (23). The energy levels are therefore labeled by J_{K_{-1},K_1} where K_{-1} represents the absolute value of K obtained by decreasing B to the prolate top limit and K_1 is the absolute value of K obtained by increasing B to the oblate limit. Since it may be shown that energy levels for a given J do not cross in going from the prolate to the oblate limit, this provides a unique labeling system. For a given J the energy matrix is of order (2J+1) with elements only along the diagonal

and removed by two above and two below the diagonal (see Eq. 2-4) (22). The matrix may be factored into four submatrices, two for K even and two for K odd. The transformation which accomplishes this factoring is known as the Wang transformation (24) and has the effect of changing from a basis set of $\langle J, K |$ to a basis set [$\langle J, K | + \langle J, -K |$].

The transition selection rules for an asymmetric rotor are $\Delta J=0,\,\pm 1$ and ΔK_{-1} and $\Delta K_{+1}=0,\,\pm 1,\,\pm 2\,\ldots$. Transitions between energy levels may be classified in several ways. Changes in J of -1, 0 or 1 take place during P, Q and R branch transitions, respectively. Further, if ΔK_{-1} is even $(0,\,\pm 2,\,\ldots)$ and ΔK_{+1} is odd $(\pm 1,\,\pm 3\,\ldots)$, the transition is termed an a-type transition. Similarly, for a c-type transition ΔK_{-1} is odd and ΔK_{+1} is even, whereas both ΔK_{-1} and ΔK_{+1} are odd for a b-type transition. The intensity of a g-type rotational transition is proportional to μ_g^2 where μ_g is the component of the total dipole moment along the molecule-fixed g axis (g=a,b) or c). The most intense transitions are those for which the K values change by 0 or \pm 1.

23 Internal Rotation

In reality molecules are not rigid rotors and the relative motions of the atoms may produce observable effects on the total rotational spectrum of the molecule. Such effects are generally classified as "vibration-rotation interactions". One such interaction exists in linear polyatomic molecules where the vibrational bending mode couples with the overall rotation causing the observed transitions to appear as doublets. This interaction is called ℓ -type doubling. Another type of interaction occurs when one part of the molecule rotates about a bond relative to the rest of the molecule. This type of motion is called torsion or internal rotation and is observed in methoxydifluorophosphine where the methyl group may rotate about the 0-C bond.

The coupling of the overall and internal rotations produces discernible effects in the rotational spectrum. These effects are usually small so that the coupling may be treated as a perturbation. The complexity of the spectrum resulting from the coupling depends on the height of the potential barrier hindering the internal rotation and on the moment of inertia of the rotating group.

A methyl group (-CH₃) is by far the most commonly studied example of a substituent undergoing internal rotation. For this case a convenient model for construction of the rotational Hamiltonian consists of a rigid symmetric top (the -CH₃ group) attached to a rigid frame which may be asymmetric. There are four degrees of freedom, three for the overall rotation and one for the internal rotation. The axis of the internal rotation must coincide with the symmetry axis of the top; however, the symmetry axis may have an arbitrary orientation with respect to the frame. Since the top is symmetric, all the structural parameters of the molecule are independent of the internal rotation.

The Hamiltonian may be expressed as (10,11),

$$H = H_r + F(p-P)^2 + V(\alpha)$$
 (2-7)

where H_r is the rigid rotor Hamiltonian Eq. (2-2) and $V(\alpha)$ is the potential function hindering the internal rotation. For internal rotation of a methyl group it has been found that to high approximation

$$V(\alpha) = 1/2 V_3(1-\cos 3\alpha)$$
 (2-8)

The remaining symbols are defined in Table 1. The second term of Eq. (2-7) may be expanded to yield,

$$Fp^2 - 2FpP + FP^2$$
 (2-9)

Table 1. Notation for Internal Rotation Problem.

- g x, y or z refers to principal axis of inertia fixed in the framework
- \boldsymbol{I}_{α} principal moments of inertia of entire molecule
- $I\alpha$ moment of inertia of internal top about its symmetry axis
- $\lambda_{f g}$ direction cosine between top axis and the principal axis ${f g}$

 $rI\alpha$ reduced moment of inertia for internal rotation where:

$$r = 1 - \sum_{g}^{2} I_{\alpha} I_{g}$$

- P_g components of the total angular momentum along the principal axes
- p total angular momentum of the internal top along its symmetry axis
- $\begin{array}{cc} P & \Sigma P \\ g & g \end{array} a^{\prod \alpha / \prod} g$
- J,M,K rotational quantum numbers
 - v the principal torsional quantum number for the harmonic oscillator limit
 - σ an index which gives the symmetry or periodicity of the torsional eigenfunction. For threefold barrier, σ = 0 for A species and σ = +1 for E species.

a taken from reference 11.

The term ${\rm Fp}^2$ is a quadratic function of ${\rm P}_g$ and hence may be incorporated directly into ${\rm H}_r$. The torsional part,

$$Fp^2 + 1/2 V_3(1-\cos 3\alpha)$$
 (2-10)

may be transformed into the Mathieu equation whose solutions are well characterized and extensively tabulated (25,26). The boundary condition, which is invariance under $\alpha \rightarrow \alpha + \frac{2\pi}{3}$, yields two solutions; the first has period $\frac{2\pi}{3}$ in α and transforms as the A species of the C_3 group, and the second has period 2π in α and transforms as the doubly degenerate E species. Thus, each torsional level consists of two sublevels which are labelled $v_A(\sigma = 0)$ and $v_E(\sigma = \pm 1)$. These levels would normally be triply degenerate due to the symmetry of the potential function. The partial lifting of this degeneracy can be considered to be a result of tunneling through the potential barrier. The rotational levels are independent of the torsional levels since the latter are not functions of the quantum numbers J and K. However, the coupling term, -2FpP, transmits an effect of the torsional motion to the rotational levels. As noted previously, the coupling terms are generally small and may be treated by perturbation theory. The coupling term is found to affect the A and E levels differently; hence, the rotational transitions appear as doublets.

The Hamiltonian of Eq. (2-7) is diagonal in J and σ but not in K or v. The elements off-diagonal in v result from the coupling term -2FpP. Approximate diagonalization in v may be obtained by applying a Van Vleck transformation (27,28). The transformed Hamiltonian may be factored into smaller submatrices $H_{\rm V}$, one for each torsional level, as follows:

$$H_{v\sigma} = H_r + F_{\Sigma}W_{v\sigma}^{(n)}p^n \qquad (2-11)$$

The zeroth order terms (n = 0 in the sum) represent the pure torsional energy, and do not affect the rotational spectrum. In addition, all the perturbation coefficients, $W_{V\sigma}^{(n)}$, for the A levels (σ = 0) vanish for n odd.

The $W_{V\sigma}^{(n)}$ depend only on the ratio V_3/F (when V_3 has the form of Eq. (2-8)) and may in principal be evaluated by nth order perturbation theory. However Herschbach (11) has shown that since the $W_{V\sigma}^{(n)}$'s are independent of the molecular symmetry, they may be evaluated in the limit of zero asymmetry, that is in the case of two coaxial symmetric tops. Koehler and Dennison (9) have shown that the internal energy levels may be written as a Fourier cosine series,

$$W_{V\sigma} = 1/4 N^{2}_{\Sigma} w \cos \ell (\theta - \theta_{0})$$
 (2-12)

where the w_{ℓ} 's are functions of the torsional level, v, and the barrier height. As the barrier height increases, the w_{ℓ} 's vanish rapidly. Further it can be shown (11) that the perturbation coefficients are related to Eq. (2-12) by:

$$W_{\mathbf{v}_{\sigma}}^{(\mathbf{n})} = \left(\frac{1}{\mathbf{n}!}\right) \left(\frac{2\pi}{\mathbf{N}}\right)^{\mathbf{n}} \left(\frac{\partial^{\mathbf{n}} W_{\mathbf{v}_{\sigma}}}{\partial \theta^{\mathbf{n}}}\right)_{\theta} = 0$$
 (2-13)

and thus to the \mathbf{w}_{ℓ} coefficients of Eq. (2-12). The utility of this method, the so-called "bootstrap" method is a result of the fact that the higher order $\mathbf{W}_{\mathbf{v}_{\sigma}}^{(n)}$'s may be written as linear combinations of the lower order \mathbf{w}_{ℓ} 's. This is because the \mathbf{w}_{ℓ} 's vanish quickly for moderate barrier heights ($\stackrel{\sim}{>}$ 1000 cal/mole), so that only a few terms from Eq. (2-12) are required.

If a representation is chosen such that $H_r + FW_{V\sigma}^{(2)}P^2$, the rigid rotor part of $H_{V\sigma}$, is diagonal, then the odd order terms will appear off-diagonal. When the separation of the rotational energy levels is large in comparison with the magnitude of the off-diagonal elements

connecting them, the odd order terms may be neglected. However, should the rotational energy levels not be widely separated, as in the case of a near symmetric top, it may be necessary to include the odd order terms (for the E levels only since $W_{VG}^{(n)} = 0$ for n odd for A levels).

As the barrier becomes lower (\lesssim 1000 cal/mole) it may become necessary to include terms to fourth order in which case Eq. (2-11) becomes:

$$H_{v\sigma} = H_r + F[W_{v\sigma}(2)(\alpha P_x + \beta P_y + \gamma P_z)^2 + W_{v\sigma}(4)(\alpha P_x + \beta P_y + \gamma P_z)^4]$$

where $\alpha = \lambda_X I \alpha / I_X$ etc. and P has been expanded (see Table I). The Hamiltonian, $H_{V_{\mathcal{O}}}$, now has terms off diagonal in K up to $\langle K | K + 4 \rangle$ (resulting from the P^4 terms). Should the barrier become very low it is necessary to treat the top as a free-rotor (29).

Koehler and Dennison (9) following Nielsen (15) have presented an alternative method of treating the internal rotor problem which employs a transformation from the principal axis system to an internal axis system in which the symmetry axis of the top is choosen as one of the coordinate axes. The purpose of this transformation is to decrease the interaction between the internal and overall rotation. Lin and Swalen (30) have reviewed the advantages and disadvantages of the various treatments of the internal rotation problem.

2.4 Stark Effect

When a static homogenous electric field is applied across the molecular sample an additional term must be included in the rigid rotor Hamiltonian to account for the interaction between the electric field and the molecular dipole moment. This term has the form (31,32),

$$H_{\varepsilon} = -\overline{\mu} \cdot \overline{\varepsilon} = -\mu \varepsilon \cos \theta$$

where $\overline{\mu}$ and $\overline{\epsilon}$ are the molecular dipole moment and electric field vectors, respectively, and $\cos \theta$ is the direction cosine between these two vectors. Since the magnitude of the interaction depends on both the dipole moment and the electric field, a convenient means of determining the dipole moment is available (7).

The presence of an electric field defines a unique direction in space along which the total angular momentum J is quantized; as M = 0, ± 1 , ± 2 , . . . $\pm J$. In the absence of an external field the energy levels are independent of M and hence M was previously omitted.

If the molecule has an average non-zero dipole moment component in the direction of the electric field, the interaction is given by the standard first order perturbation result,

$$E_{j}^{(1)} = \langle \psi_{j}^{(0)} | H_{\varepsilon} | \psi_{j}^{(0)} \rangle$$

and has the form,

$$E^{(1)} = -\frac{\mu \epsilon KM}{J(J+1)} \qquad (2-14)$$

It can be shown (7) that such a nonzero dipole component will exist only in the presence of degenerate energy levels, a condition which is satisfied for symmetric top molecules due to the degeneracy in K (see Eqs. 2-5 and 2-6).

If the molecule does not possess an average nonzero component, the electric field may induce one and produce a second order stark effect. The second order interaction, which is normally much smaller than the first order effect, may be calculated from the standard second order perturbation results:

$$E^{(2)} = \sum_{i \neq j} \frac{\langle \psi_{j}^{(0)} | H_{\varepsilon} | \psi_{i}^{(0)} \rangle \langle \psi_{i}^{(0)} | H_{\varepsilon} | \psi_{j}^{(0)} \rangle}{(E_{j}^{(0)} - E_{j}^{(0)})}$$
(2-15)

The $<\psi_{\mathbf{j}}^{}(0)|_{\mathbf{H}_{\varepsilon}}|_{\psi_{\mathbf{j}}^{}}(0)>$ are the dipole matrix elements, multiplied by the electric field, in the asymmetric rotor representation which diagonalized the energy matrix. The transformations required to bring the asymmetric rotor dipole matrix elements into this form are available from the solution of the energy level problem. The required direction cosine matrix elements have been given in a convenient form by Schwendeman (33).

Since H_{ϵ} is proportional to μ and ϵ , $E^{(2)}$ will be proportional to their squares. Substitution of the appropriate dipole matrix elements into Eq.(2-15) and summation gives the result that $E^{(2)}$ may be written as a sum of two terms (7),

$$E_{J_{K_{-1},K_{+1}}}^{(2)} = \sum_{g} (A_{gJ_{K_{-1},K_{+1}}} + M^{2}B_{gJ_{K_{-1},K_{+1}}})_{\mu_{g}}^{2} \epsilon^{2}$$
 (2-16)

where g = a, b or c. The second order Stark effect will exist for asymmetric rotors (the K degeneracy has been lifted) unless accidental near-degeneracies exist between energy levels.

A molecular rotational resonance spectrometer employing stark modulation was first described by Hughes and Wilson (5). The basic principle involves modulation of the absorption signal by application of a periodic electric field across the sample.

The Stark effect is also very useful in assigning transitions. From Eq. (2-16) it can be seen that the perturbation energy is a function of M^2 , in addition to μ and ϵ . Therefore, application of a sufficiently large Stark field will split a particular energy level into J+1 components. When the Stark field is parallel to the microwave radiation electric field, the selection rule for M is $\Delta M=0$. The intensity of the components is given by $J^2_{upper}-M^2$ (except for M=0 when it is 1/2 J^2_{upper}) for an

R-branch transition and by M^2 for a Q-branch transition. Thus an R-branch transition $(J \to J+1)$ will exhibit J+1 components, while a Q-branch transition $(J \to J)$ will exhibit only J components. Therefore, the value of J_{lower} for a transition may be determined by counting the number of Stark components, and the characteristic intensities of the components identify the transition as Q or R-branch.

2.5 Molecular Structure

As shown previously, Section 2.1, the rotational energy levels and hence the transition energies are completely determined by the three rotational constants A, B and C, which are inversely proportional to the corresponding principal moments of inertia. Since the moments of inertia are sums of products of atomic masses and molecular coordinates; changing the mass at one of the atomic positions by means of isotopic substitution moves the center of mass and changes the moments of inertia of the molecule. If the assumption is made that isotopic substitution does not alter the molecular structure, it is then possible to relate the differences in the principal moments of inertia of the isotopically substituted and normal molecules to the coordinates of the substituted atom relative to the center of mass of the normal molecule.

Kraitchman (13) has shown that in the case of an asymmetric molecule the relationships are easily developed from the principal second moments of inertia which are defined as:

$$P_{x} = 1/2(-I_{x} + I_{y} + I_{z}) = \sum_{i=1}^{m} i^{x}i^{2}$$

$$P_{xy} = \sum_{i=1}^{m} i^{x}i^{y}i^{2} = 0$$
(2-17)

with the remaining terms obtained by cyclic permutation of x, y and z. In the substituted molecule these moments become:

$$P_{xx}' = P_{x} + \mu x^{2}$$

$$P_{xy}' = \mu xy \quad \text{etc}$$
(2-18)

where $_{\mu}$ = M $_{\Delta}$ m/(M+ $_{\Delta}$ m), M is the mass of the normal molecule, and $_{\Delta}$ m is the change in mass due to substitution. These new second moments are now the elements of an inertial tensor:

$$P_{x} + \mu_{x}^{2}$$
 μ_{xy} μ_{xz}

$$P_{y} + \mu_{x}^{2} \quad \mu_{y}^{y}z$$

$$P_{z} + \mu_{z}^{2}$$
(2-19)

It is known that definite relationships exist between the coefficients of a cubic equation and its roots. For example, if P_x ', P_y ' and P_z ' are the roots of a cubic equation in P', then:

$$P^{3} - (P_{x} + P_{y} + P_{z})P^{2} + (P_{x} + P_{y} + P_{y} + P_{z} + P_{z} + P_{x})P^{2} - P_{x} + P_{y} + P_{z} = 0$$

If the secular equation of Eq. (2-19) is expanded and the corresponding coefficients are equated to those in the above expression, three equations in x^2 , y^2 and z^2 may be obtained. Solution of these equations yields,

$$|x| = \left\{ \frac{1}{2\mu} \left[(I_{y}' - I_{y}) + (I_{z}' - I_{z}) - (I_{x}' - I_{x}) \right] \right.$$

$$X[1 + \frac{(I_{x}' - I_{x}) - (I_{y}' - I_{y}) + (I_{z}' - I_{z})}{2(I_{x} - I_{y})} \right] \qquad (2-20)$$

$$X[1 + \frac{(I_{x}' - I_{x}) + (I_{y}' - I_{y}) - (I_{z}' - I_{z})}{2(I_{y} - I_{z})} \right]$$

where Eq. (2-17) have been used to put the expression into the form involving the principal moments of inertia. Expressions for y and z are obtained by cyclic permutation of the subscripts. Thus, in principal, to obtain a complete molecular structure one needs only to make an isotopic substitution at each atomic position and employ Eq. (2-20) to determine the atomic coordinates relative to the center of mass of the original molecule.

In some cases it may be impractical or impossible (synthesis very difficult or no stable isotope available) to substitute isotopically at each position. In such cases the nine independent moment equations, i.e., the three principal moments of inertia, three products of inertia, and the three center of mass equations, may be used to calculate the coordinates for three atoms (14). Thus for a general asymmetric rotor of N atoms only N-3 atoms must be isotopically substituted. If the molecule has some symmetry, such as a plane of symmetry, fewer substitutions will be required since the symmetrically related atoms form a redundant set. This is the case for methoxydifluorophosphine where only three substitutions are required to determine the positions of eight atoms.

III. EXPERIMENTAL

3.1 Introduction

Molecular Rotational Resonance Spectroscopy shares many of the general characteristics usually associated with other forms of spectroscopy. A klystron or backward wave oscillator (BWO) serves as a source of microwave radiation which passes through an absorption cell, usually constructed of brass X-band waveguide, containing the sample. The signal is monitored by a crystal diode detector and amplified by a tuned preamplifier-phase sensitive detector combination. The resulting amplified signal is then displayed either by an oscilloscope trace or strip chart recorder. A simplified block diagram of a typical MRR spectrometer is shown in Figure I.

The MRR spectrometers on which this work was done are typical Hughes-Wilson (5) stark modulated spectrometers of 33 1/3, 90 and 100 kHz⁽¹⁾ modulation frequencies. The 33 1/3 kHz instrument is a Hewlett-Packard model 8460 A R-band spectrometer (26,500 to 40,000 MHz) while the others are of conventional design. The characteristics and operation of these spectrometers have been presented elsewhere (34-37), therefore only a brief description of the major components which differ from typical spectrometers and experimental conditions will be discussed here.

^{(1) 1} Hz = 1 sec⁻¹; 1 kHz = 10^{3} Hz; 1 MHz = 10^{6} Hz; 1 GHz = 10^{9} Hz

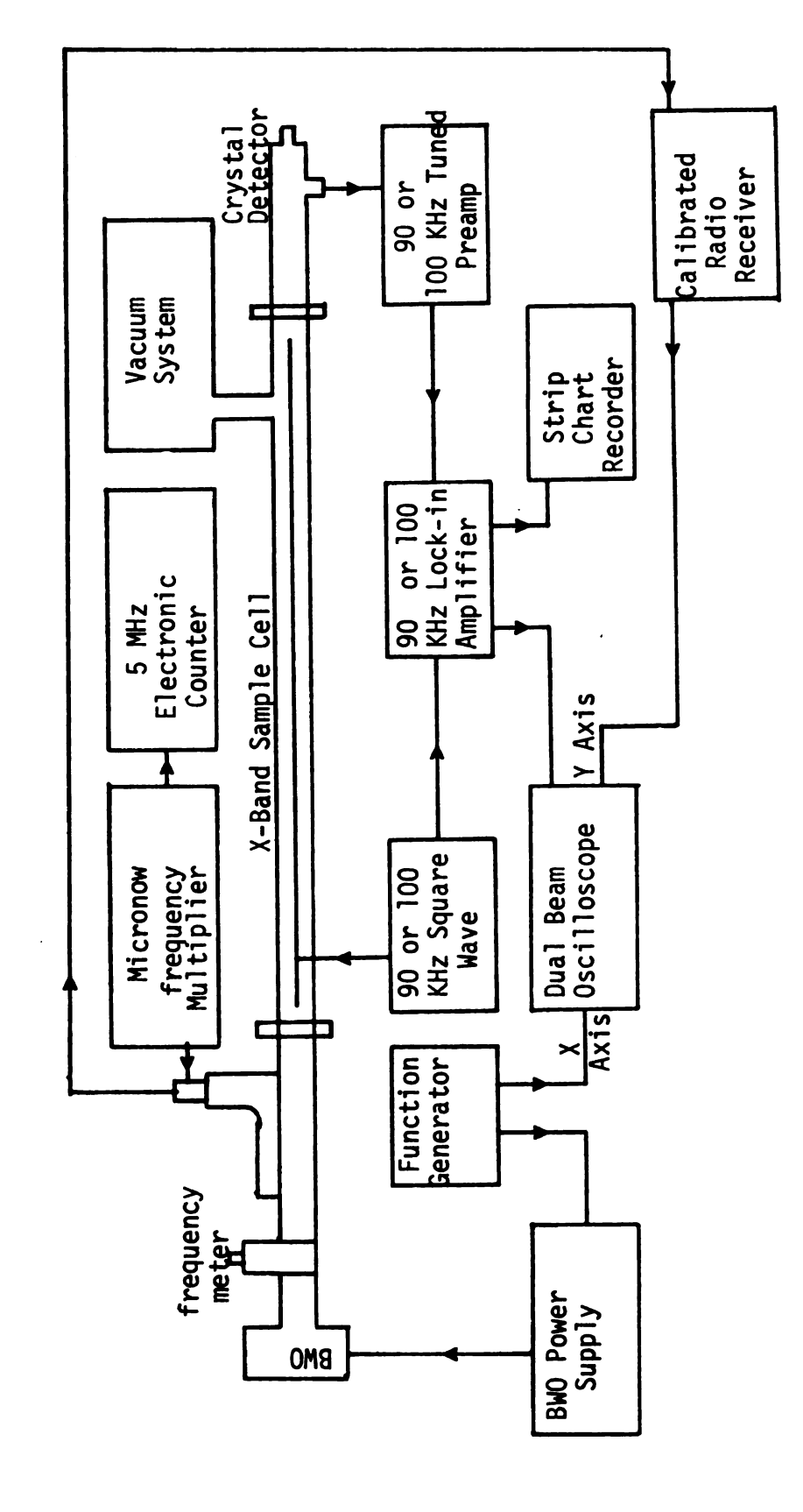
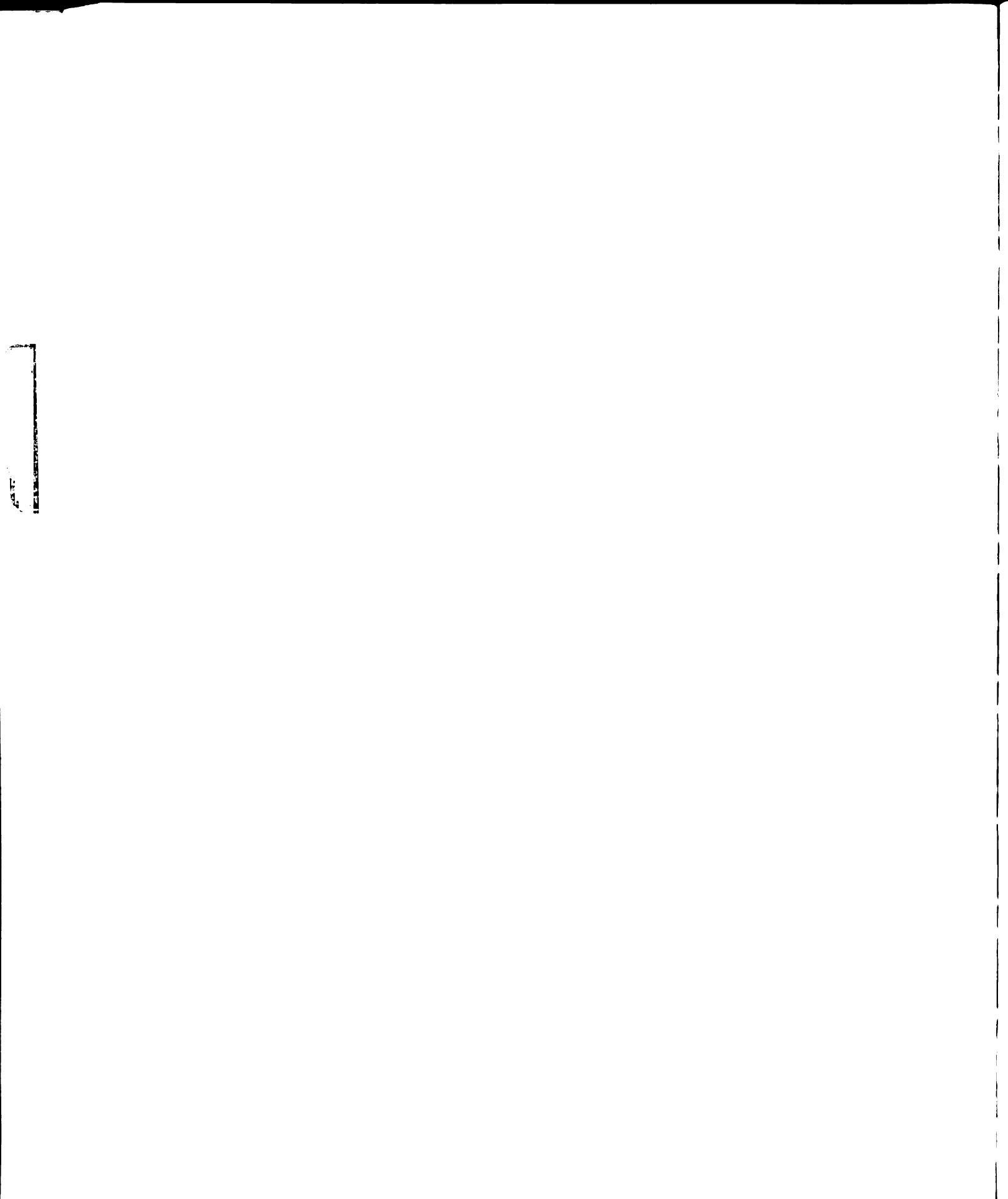


Figure 1. Block diagram of a typical MRR spectrometer.



3.2 Radiation Sources

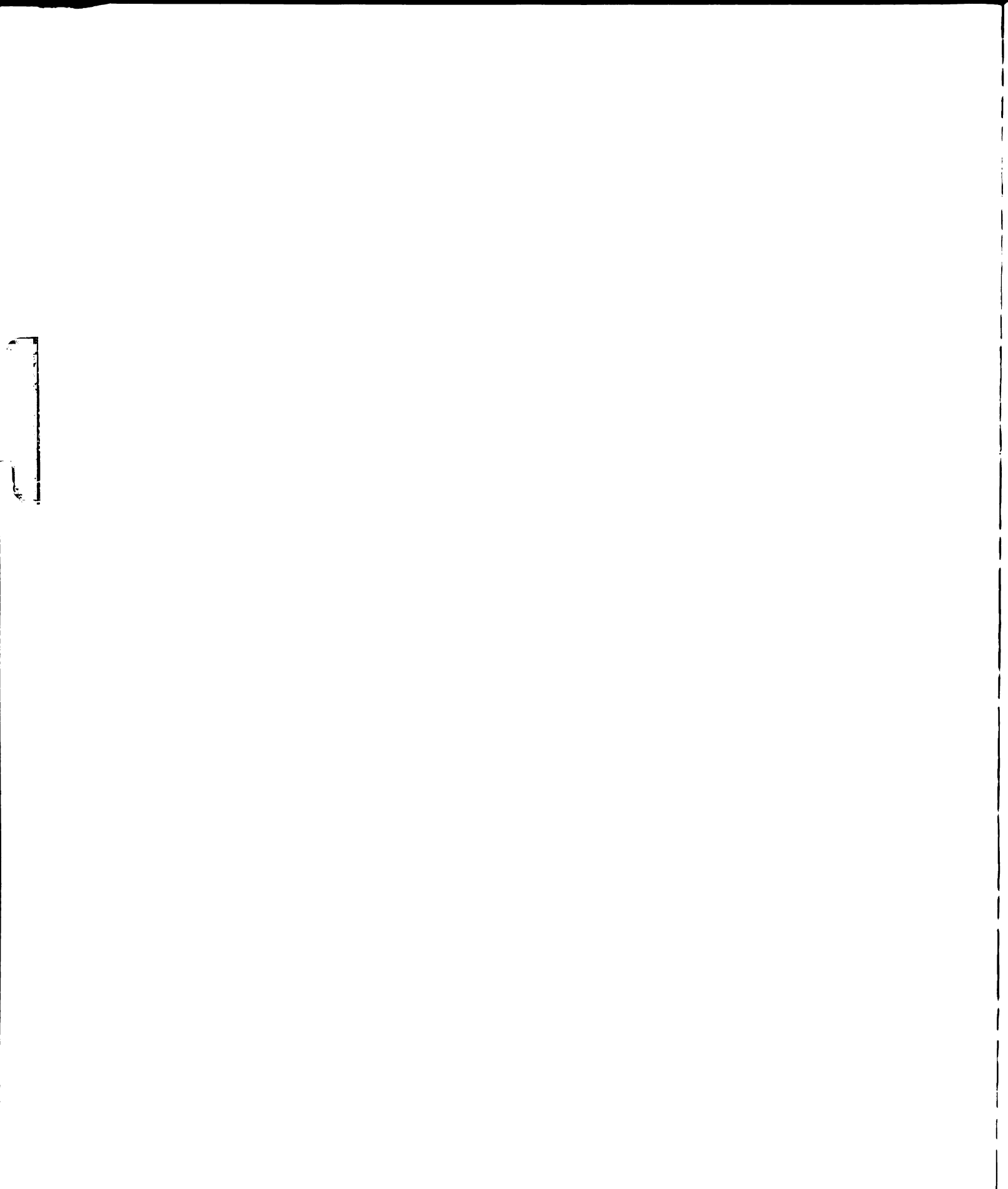
While klystrons have been the microwave sources of choice in the past, recent advances in Backward Wave Oscillators (BWO's) coupled with a decreasing initial investment have made them extremely attractive.

Klystrons require simultaneous adjustment of the reflector voltage and resonant cavity size to maintain optimum operating conditions while tuning the oscillation frequency. It is this feature which makes recording a spectrum with a klystron tedious. However, the frequency of a BWO is dependent only on the voltage applied to the helix of the tube. Thus, varying the helix voltage provides a very convenient means of sweeping the frequency. At Michigan State University the BWO frequency is varied by adding a small amplitude, low frequency sawtooth or triangular wave to a constant helix voltage. A Wavetek model 112578 function generator supplies the variable voltage and at its maximum output of 30 volts provides 150 to 750 MHz sweep widths, depending on the frequency of the BWO.

3.3 Spectral Display

Spectra may be displayed either on a strip chart recording or an oscilloscope. The latter is usually used in these laboratories. However, recording the spectra is more desirable when greater sensitivity or higher resolution are required. The Hewlett-Packard spectrometer is designed for recording tracing only.

All the frequency and Stark effect measurements for vinylcyclopropane and methyldifluoro-phosphine were made using oscilloscope display with the exception of the ¹³C (in natural abundance) measurements in vinylcyclo-propane and the intensity measurements in methyldifluorophosphine. All the measurements on methyldifluorophosphine were made with the Hewlett-Packard spectrometer and recorder display.



3.4 Sample Pressure and Temperature

Sample pressures are normally monitored using a RCA 1946 thermocouple tube. This method does not provide absolute pressure measurements but does provide a means for approximately reproducing the sample pressure from experiment to experiment. A Baratron type 77 vacuum gauge equipped with a 1 mm Hg pressure head is available for absolute pressure measurements when required.

Measurements with the Baratron gauge indicate that the studies on vinylcyclopropane were done in the 15-25 micron range, methyldifluorophosphine in the 8-15 micron range and methoxydifluorophosphine in 40-80 micron range.

Sample temperatures are normally maintained at -78°C by packing dry ice around the sample cell. Should the sample vapor pressure be too low at this temperature a refrigeration unit is available which is capable of maintaining temperatures from room temperature to -15°C.

All spectral measurements in this study were made at -78°C unless otherwise noted.

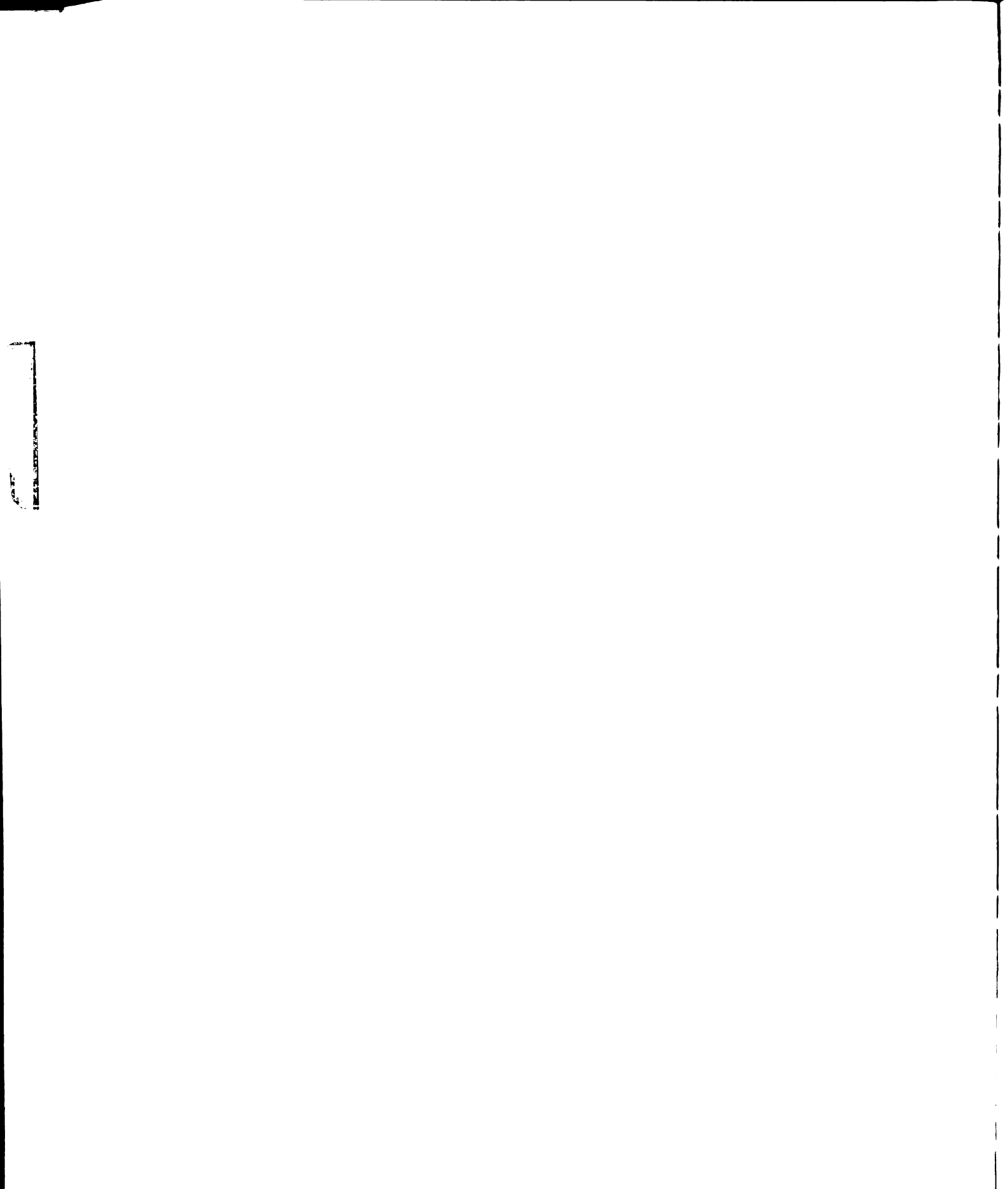
3.5 Frequency Measurements

Rotational transition frequency measurements were made in a conventional manner (34) with an absolute accuracy of ±.05 MHz. The local oscillator to which the experimental frequencies are referenced is a 1 MHz quartz crystal controlled oscillator. (1) This oscillator is periodically compared to one of the carrier frequencies of the National Bureau of Standards Radio Station WWV.

⁽¹⁾ Manson Laboratories RD-140A.

Although strip chart recording is a common means of displaying a spectrum, placing accurate frequency markers on the recording has been a persistent problem. In this laboratory a Hewlett-Packard electronic counter, model 5245L, equipped with a Hewlett-Packard transfer oscillator, model 5257A, is available. This combination provides direct and continuous frequency measurements from 8,000 to 18,000 MHz. The counter is equipped with an output which provides a binary representation of each digit of the displayed frequency measurement. A binary decoder was designed by the author and constructed in the Chemistry Department Electronics Shop. The decoder monitors the binary frequency representation and provides a voltage pulse to drive an events marker on the recorder each time the binary representation meets certain preset conditions, e.g., at preset frequency intervals. By this means frequency markers are available in intervals varying 2 kHz to 1 GHz. For most recording purposes intervals of 1, 2, 5 and 10 MHz are sufficient. A complete description of the decoder is given in Appendix I.

The Hewlett-Packard spectrometer automatically provides frequency markers on the spectral recordings at a selected interval from 1 kHz to 10 MHz.



IV. MOLECULAR ROTATIONAL RESONANCE SPECTRUM OF TRANS-VINYLCYCLOPROPANE

4.1 Introduction

In the past several years rotational resonance studies of several cyclopropyl derivatives have been undertaken in these laboratories.

Results of studies of cyclopropanecarboxaldehyde and cyclopropanecarboxylic acid fluoride were recently reported by Volltrauer and Schwendeman (38,39). The torsional potential constants were evaluated for both molecules and discussed in terms of being the net result of electronic effects of the orbitals of the axial atoms and steric effects of the nonbonded atoms.

Another study, by Lee (40) on methyl cyclopropylketone, has just been completed. Unfortunately, in this case only the cis configuration (oxygen cis to the ring) could be assigned and therefore the torsional potential function could not be completely evaluated. A study of vinylcyclopropane was undertaken because it appeared that this compound would be an excellent example from which to obtain additional information concerning the theoretical interpretation of torsional potential constants in cyclopropyl compounds.

Luttke and de Meijere (41) have reported results of NMR studies which indicate that vinylcyclopropane exists in two configurations: a cis form (θ = 0°, the vinyl group cis to the ring) and a trans form (θ = 180°). Variable temperature studies of the equilibrium coefficient, $K = \frac{X_{trans}}{X_{cis}}$, indicate that the trans form should be energetically favored by

1.1 \pm 0.2 kcal/mole. In a more recent electron diffraction study Luttke and de Meijere (42) report that at 20°C vinylcyclopropane consists of trans and gauche (θ = 60-70°) comformers in a 3:1 ratio with the trans form being more stable by 1.1 \pm 0.2 kcal/mole.

The spectrum of vinylcyclopropane is rather sparse, and transitions in molecules in the ground and first three excited torsional states of the trans configuration were definitely assigned. However, an exhaustive search failed to disclose any transitions assignable to the cis or any other configuration. The dipole moment of the trans configuration was determined.

The sample of vinylcyclopropane was obtained from Chemical Samples Company, Columbus, Ohio, and was used without further purification.

4.2 The Rotational Constants

The first approximation to the principal moments of inertia and the corresponding rotational constants were calculated assuming the molecular parameters given in Table 2. The calculations were facilitated by the computer program STRUCT which had been written by Dr. R. H. Schwendeman. This program locates the molecular center of mass and then diagonalizes the resulting inertial tensor. The diagonalization transforms the initial axis system into the principal axis system. In addition, STRUCT calculates the atomic coordinates in the principal axis system. The results of this calculation for trans-vinylcyclopropane are given in Table 3 and the projection of the molecule on the molecular symmetry plane, the a-c inertial plane, is shown in Figure II. Since the b axis is perpendicular to the molecular plane of symmetry, the b component of the dipole moment, μ_b , will be zero; therefore, only a and c-type transitions should be observed. The calculated rotational constants also indicate that this

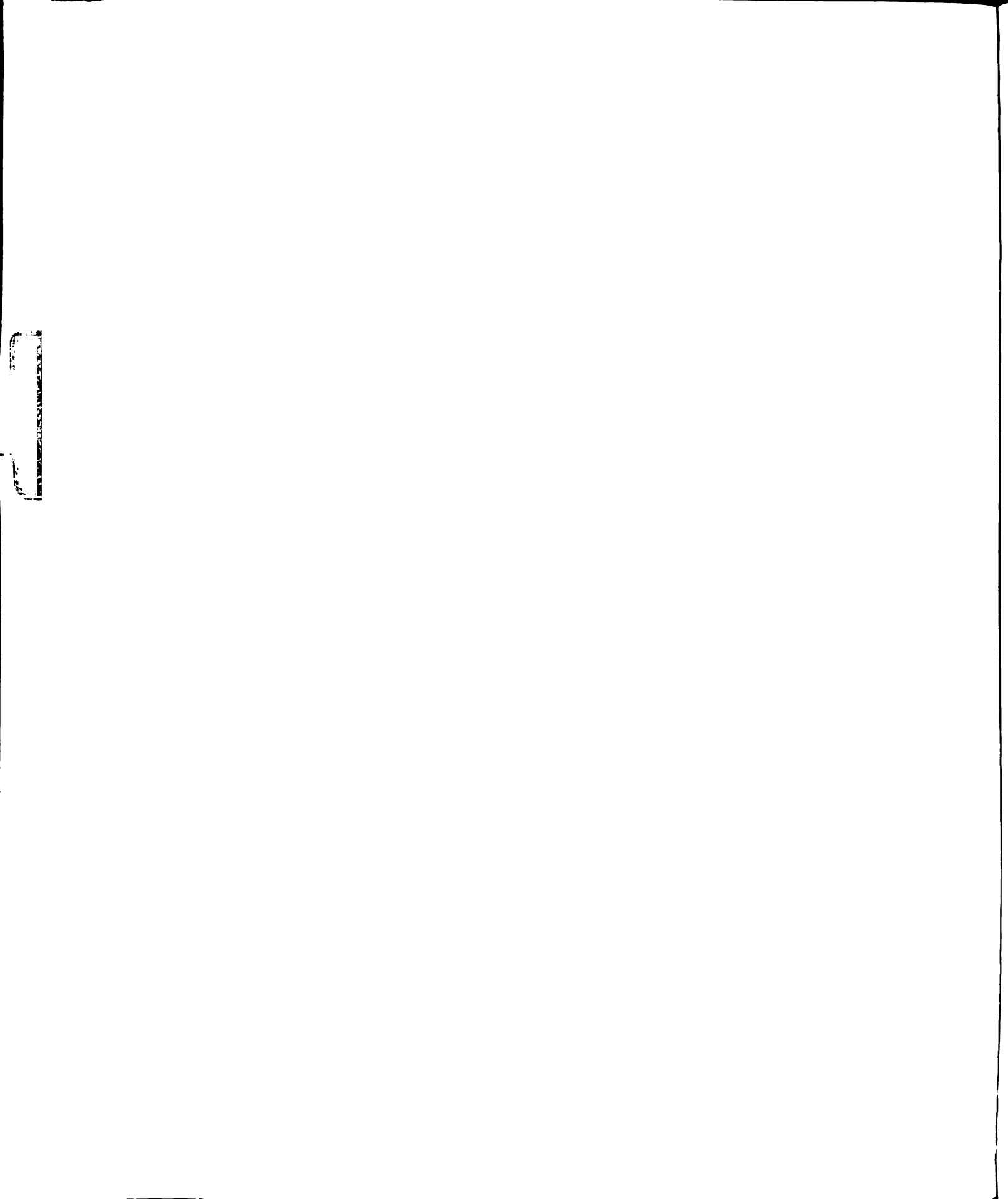
Table 2. Assumed Molecular Parameters for Trans-Vinylcyclopropane.

r(CH)	= 1.08 Å	< (c ₁ c ₅ c ₁₀) = 125°
r(CC)	= 1.52 Å	$< (H_{12}C_{10}H_{13}) = 117^{\circ}$
r(C ₅ H ₁₀)	= 1.34 Å	$< (H_6 C_2 H_7) = 116^{\circ}$
r(C ₁ H ₅)	= 1.50 Å	$< (H_{11}C_5C_{10}) = 121^{\circ}$

Table 3. The Atomic Coordinates^a and Rotational Constants of Trans-Vinylcyclopropane in the Principal Axis System Using the Assumed Parameters of Table 2.

\tom	a	b	С
 ² 1	-0.244	0.000	-0.442
2	-1.453	0.760	0.078
² 3	-1.453	-0.760	0.078
² 5	0.989	0.000	0.412
² 10	2.215	0.000	-0.128
14	-0.078	0.000	-1.519
¹ 6	-1.352	1.260	1.041
7	-2.083	1.260	-0.656
8	-1.352	-1.260	1.041
9	-2.083	-1.260	-0.656
11	0.844	0.000	1.482
12	3.103	0.000	0.486
13	2.360	0.000	-1.198
	A = 1493	6. MHz	
	B = 304	3. MHz	
	C = 292		

a Coordinates are in Angstroms.



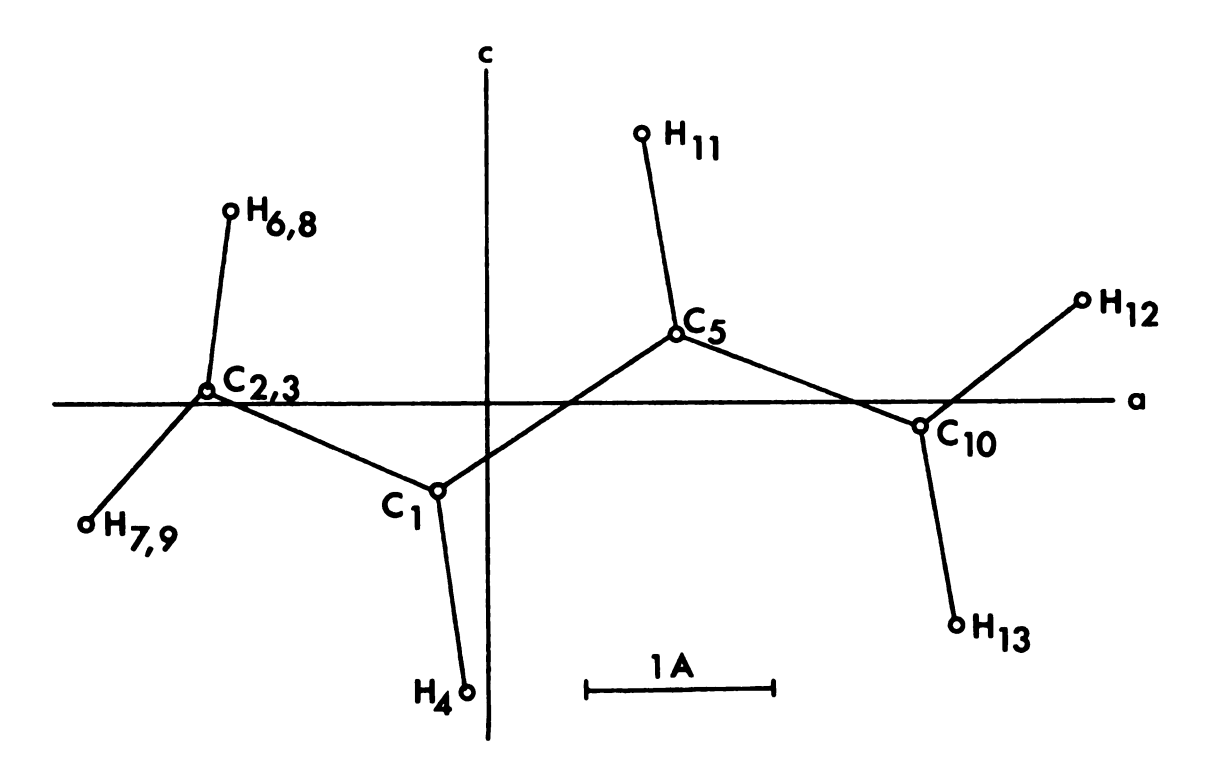


Figure II. The projection of trans-vinylcyclopropane onto the molecular symmetry plane.

conformation is a near prolate symmetric top (B approximately equals C and both are much smaller than A). Thus, the a-type transitions should appear in closely spaced groups approximately separated by (B + C).

The preliminary rotational constants were used to calculate rotational energy levels and transition frequencies. These calculations were performed by the computer program EIGVALS which was written by Hand and Schwendeman (43).

With only rotational constants, quadrupole coupling constants and dipole moments as input data the EIGVALS program calculates the rotational energy eigenvalues, quadrupole coupling energies, transition frequencies, line strengths and Stark effect coefficients for a rigid asymmetric rotor.

The Hamiltonian matrix elements are generated from the appropriate Wang symmetric rotor basis functions (depending upon whether the molecule is a near oblate or prolate top). The energy matrix is then diagonalized by a continued fraction method to yield the rotational energy level eigenvalues which in conjunction with the appropriate selection rules result in the transition frequencies. The matrices of the coefficients of the diagonalizing transformation (T matrices) are also generated and stored.

The line strength for each transition is calculated by transforming the appropriate direction cosine matrix elements (33,44) to the proper asymmetric rotor representation using the previously determined T matrices. The resulting line strengths are then used to calculate transition intensities which are very useful in assigning the spectrum.

The Stark effect coefficients are calculated by second-order perturbation theory from the line strengths and energy levels. The coefficients are further multiplied by the appropriate squared dipole

moment components and by a factor which insures that the resulting coefficients have units of Hz $(volt/cm)^{-2}$. These coefficients are then used to predict the Stark effect for any transition, which is extremely useful for spectral assignments.

A search of the spectral regions predicted by EIGVALS disclosed groups of transitions which were approximately separated by B + C as expected for a-type transitions. Since each group involved transitions whose J quantum numbers had increased by one - i.e., the first group would be J = 1-2, the second J = 2-3, etc. - the gross assignment of the spectrum was straightforward. Individual transitions within a group were assigned to the proper rotational quantum numbers by making use of the relative position of each transition in the group, the relative intensities of each and the Stark effects.

Although the preliminary calculations indicated that the spectrum should consist of a and c-type transitions for the trans configuration, only a-type transitions were observed. The observed and calculated frequencies of the assigned transitions are compared in Table 4. Because trans-vinylcycloproprane is a near prolate symmetric top the frequencies of the a-type R-branch transitions which were assigned are only slightly dependent on the A rotational constant. This makes an accurate determination of A from these frequencies impossible. However, the observation and subsequent analysis of a peculiar Stark effect for the $|\mathbf{M}|=1$ component of the 2_{02} - 3_{03} transition made a somewhat more accurate determination of the A rotational constant possible. The analysis of this Stark effect will be discussed below.

The low J transitions, $J = 1 \rightarrow 2$ and $J = 2 \rightarrow 3$, were used in a least squares analysis to determine the rotational constants and moments of inertia which are given in Table 5. The final rotational constants are

Comparison of Observed and Calculated^a Frequencies^b for the Ground and First Three Excited Torsional States of Trans-Vinylcyclopropane. Table 4.

Transition	0 = ^	\ 	v = 2	v = 3
101-202	12004.64(4.61)	12029.99(9.90)		
111-212	11885.44(5.44)	11903.60(3.51)		
110-211	12125.54(5.58)	12158.41(8.32)		
202-303	18004.72(4.68)			
212-313	17827.57(7.60)			
303-404	24002.00(2.06)	24053.84(1.73)		
313-414	23768.99(9.09)		23840.84(0.71)	
312-413	24249.20(9.36)			
322-423	24010.01(0.32)	24060.90(1.04)		
321-422	24018.91(9.28)			
3 ₃₀ -4 ₃₁	24012.07(2.82)			
404-505	29995.72(5.87)	30057.05(7.11)	30117.72(7.83)	30177.06(7.42)

Table 4 (Continued)

	0	\ 	< = 2	e = >
414-515	29709.50(9.72)	29754.32(4.40)	29798.84(8.81)	29842.29(2.18)
413-514	30309.71(9.99)	30391.32(1.32)	30472.21(2.08)	
423-524	30011.29(1.78)	30074.74(5.03)	30137.72(7.87)	30199.51(9.69)
422-523	30029.12(9.69)	30095.08(5.21)	30160.66(0.42)	30225.19(4.75)

a Last three digits of calculated frequencies are in parenthesis.

b In MHz.Measured frequencies are $\pm .05$ MHz.

Table 5. Rotational Constants^a and Principal Moments of Inertia^b for the Ground and First Three Excited Torsional States of Trans-Vinylcyclopropane.

	v = 0	v = 1	v = 2	v = 3
Α	15050.			
В	3061.41	3071.43	3081.38	3091.22
С	2941.34	2944.02	2946.70	2949.27
Ia	33.57980			
I _b	165.07932	164.54092	164.00973	163.48734
I _c	171.81818	171.66157	171.50585	171.35618

a In MHz. Uncertainties are as follows: A, ± 15 MHz; B, ± 0.05 MHz; C, ± 0.05 MHz.

b In $u \cdot \mathring{A}^2$. Assumed conversion factor of 505376.($u \cdot \mathring{A}^2$)(MHz).

quite close to those predicted by STRUCT (see Table 3) which supports the premise that the assigned transitions are due to the trans-configuration of vinylcyclopropane.

A search for vibrationally excited states revealed that each transition is followed at higher frequency by a series of approximately equally spaced, progressively weaker transitions which exhibit Stark effects which are identical with the main transition. The intensities of these transitions decrease by a factor of approximately 2.5 between successive excited states which indicates a vibrational excitation energy of approximately 125 cm⁻¹. Presumably the only vibration present in vinylcyclopropane having this low an excitation energy is the out-ofplane torsion of the vinyl group about the carbon-carbon bond. A comparable value of 100 cm⁻¹ has been obtained by Volltrauer (45) for cyclopropanecarboxaldehyde. Although as many as five excited states were observed, frequencies were measured for only the first three states because of the rapid decrease in intensity. The assigned transitions along with the observed frequencies are given in Table 4, and the derived rotational constants and principal moments of inertia are given in Table 5. The linear plot of the rotational constants vs.v, as shown in Figure III, provides evidence that the potential function hindering the torsional motion is essentially harmonic.

An extensive search for transitions which could be assigned to the cis or to some gauche configuration proved unsuccessful. All unassigned transitions in the spectrum are at least a factor of ten lower in intensity than transitions assigned to the trans configuration. There are three possible explanations for this result. First, the molecular population of any other configuration may be very small; second, the dipole moment of any other configuration may be very small, and third, some combination of these.

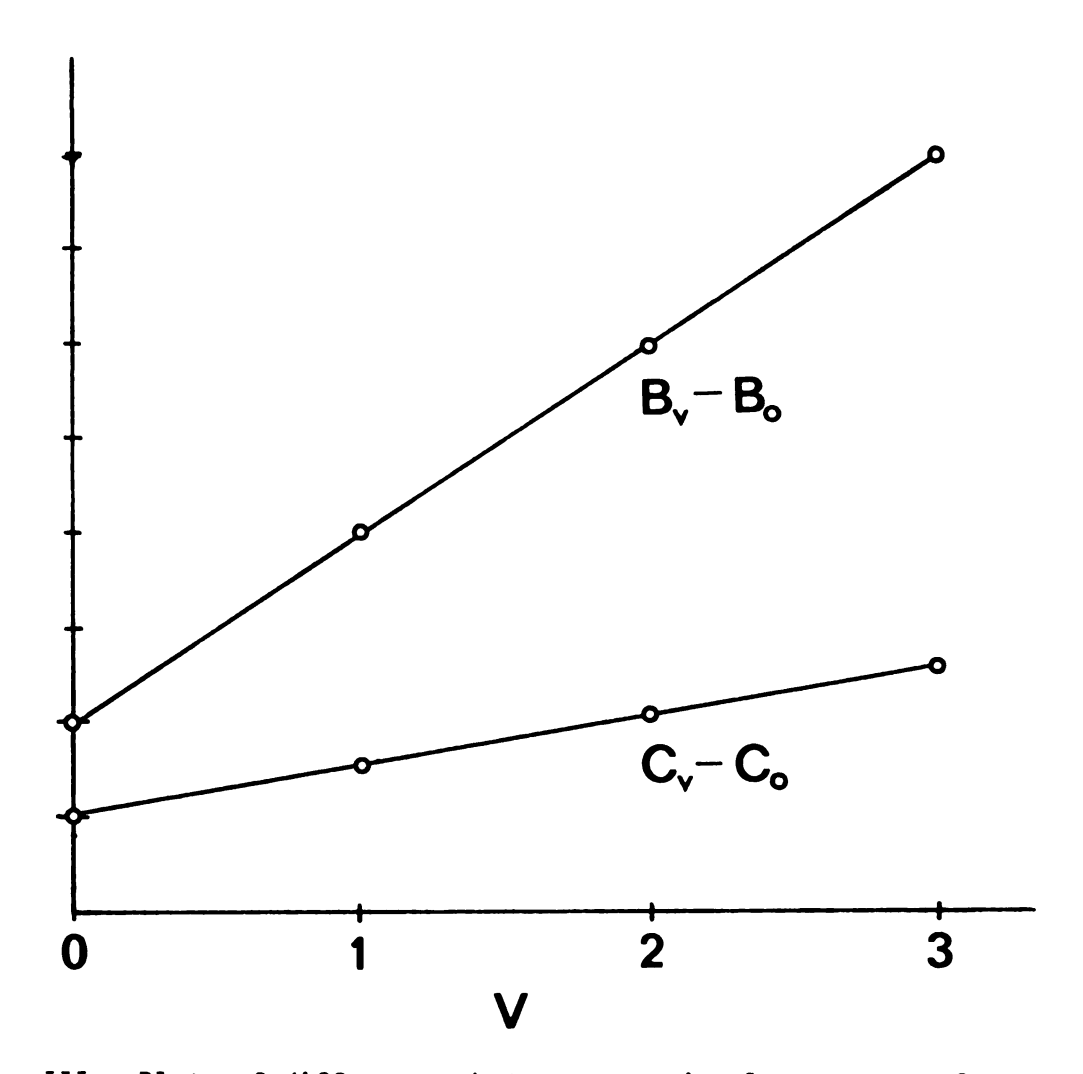


Figure III. Plots of differences between rotational constants of transvinylcyclopropane in the vth torsional state and the ground vibrational state as a function of v. The vertical scale is marked in units of 5 MHz.

The search for a second configuration did disclose transitions which were assigned to a naturally occurring molecular species having ^{13}C substituted at one of the ring positions C_2 or C_3 . Since these positions are equivalent, the intensity of the transitions was twice that of transitions resulting from other ^{13}C species. The assigned transitions and their measured frequencies are given in Table 6 and the derived rotational constants are given in Table 7. No attempt was made to assign transitions belonging to other ^{13}C species since they were predicted to occur in regions having a high density of normal species transitions.

4.3 Dipole Moment

The molecular dipole moment may be calculated from Eq. (2-16) provided that the displacements, Δv , of the Stark components from the zero-field transition can be measured as a function of the applied electric field ε . The coefficients A_J and B_J were calculated by EIGVALS as mentioned previously.

Values of Δv <u>vs.</u> ϵ were determined for the M = 0 components of the three $J=1\to 2$ transitions and the M = 0 component of the 2_{02}^{-3} transition. The slopes, $\partial v/\Delta \epsilon^2$, were used with Eq. (2-16) to calculate the three components of the dipole moment by a least squares analysis. As expected, the out of plane component, μ_b , was zero within experimental error. The μ_a and μ_c components were then recalculated with μ_b set equal to zero with the result that their values were not significantly changed from the previous calculation. The resulting values of μ_a , μ_c and $\mu_T(\mu_T^2 = \mu_a^2 + \mu_c^2)$ are given in Table 8 along with a comparison of the experimental and calculated values of the slope. Table 9 shows a comparison of reported dipole moments for some related hydrocarbons.

Table 6. Comparison of Observed and Calculated^a Frequencies^b for a 13C Species of Trans-Vinylcyclopropane.

Frequency
23666.5(6.58)
23927.0(6.89)
29575.7(5.83)
29275.9(5.74)
29906.8(6.73)
29593.1(3.36)

a Last three digits of calculated frequencies are in parenthesis.

Table 7. Rotational Constants a and Principal Moments of Inertia b for the ^{13}C species of Trans-Vinylcyclopropane.

A	15050.
В	3022.66
С	2896.45
Ia	33.57980
I _b	167.19555
Ic	174.48141

a In MHz. Uncertainties are as follows: A, ± 15 MHz; B, $\pm .1$ MHz; C, $\pm .1$ MHz.

b In MHz. Measured frequencies are +0.15 MHz.

b In $u \cdot \mathring{A}^2$. Assumed conversion factor of 505376.($u \cdot \mathring{A}^2$)(MHz)

Table 8. The Stark Effect and Dipole Moment of Trans-Vinylcyclopropane.

Transition	M	$\frac{\partial v}{\partial \varepsilon^2}$ obs	_{θν} a ^{θε 2} calc
111-212	0	5.64	5.82
1 ₀₁ -2 ₀₂	0	-10.21	-10.13
110-211	0	2.34	2.25
² 02 ⁻³ 03	0	2.17	2.14
	$\mu_a = 0.4$	86 <u>+</u> 0.007 D	
	$u_b = 0.0$	D	
	$\mu_{C} = 0.1$	10 <u>+</u> 0.003 D	
	$\mu_T = 0.4$	98 <u>+</u> 0.007 D	

a Hz/(volt/cm)² assuming $\mu_{OCS} = 0.7152$ D.

b Uncertainty in observed slopes is \pm 1.0%.

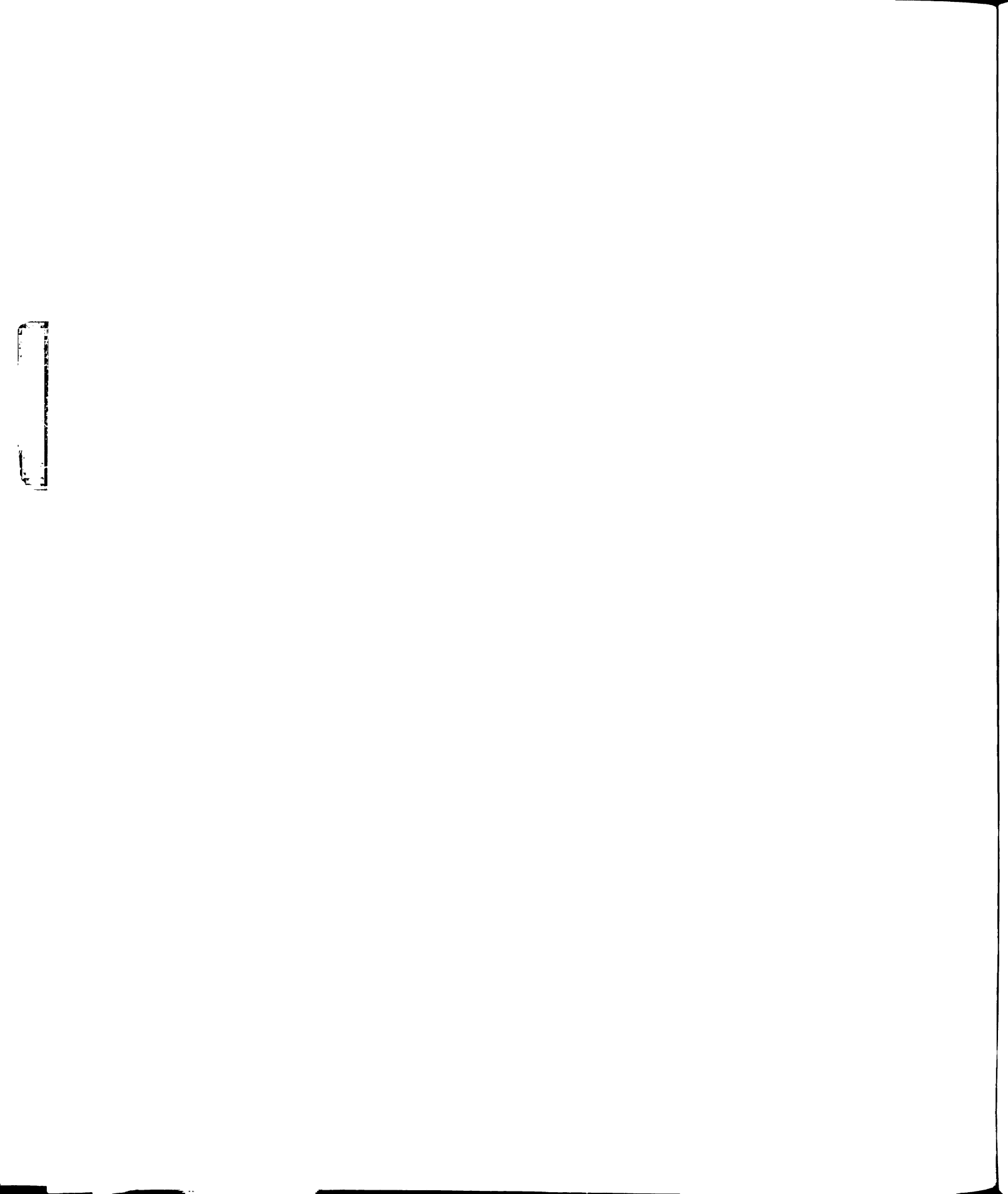


Table 9. Comparison of Dipole Moments of some Related Hydrocarbons.

Compound	μŢ ^a	Ref.
Propylene	0.364	46
Isobutene	0.503	47
Methyl-allene	0.401	48
Isoprene	0.25	49
trans-Vinylcyclopropane	0.498	this work

a The total dipole moment in Debyes.

Since the intensities of MRR transitions are directly proportional to the square of the dipole moment components the ratio of $\mu_a^2:\mu_c^2$ of 19.5 offers an explanation for the failure to observe c-type transitions. This ratio indicates the c-type transitions would only be 5% as intense as the a-type transitions. As mentioned previously, the strongest unassigned transitions are at least a factor of ten weaker than the a-type transitions.

4.4 The Anomalous Stark Effect of the |M| = 1 Component of the 2_{02} - 3_{03} Transition

As was discussed in Chapter II, the Stark effect in an asymmetric rotor normally possesses a quadratic dependence on the electric field ε and may be treated by second order perturbation theory. However, when one or more of the energy differences in the denominator of Eq. (2-15) becomes small, the necessary conditions for a second order perturbation treatment are no longer met and a direct calculation is required. This situation commonly exists for near symmetric tops because the energy difference between asymmetry doublets is small.(1) In the present case a third energy level, the 2_{02} level, is near both the 1_{10} and 1_{11} levels and for |M|=1 a perturbation connection exists between the 2_{02} and the 1_{10} , 1_{11} levels. Although there is no direct connection between the 2_{02} and 1_{11} levels, (2) the 2_{02} level is perturbed by its proximity to the 1_{10} and 1_{11} levels. If the dipole moment components in Table 8, which were obtained using M components exhibiting normal quadratic Stark

l. For a near symmetric prolate top the asymmetry doublets consist of the pairs of energy levels having near maximum and equal values for K_{-1} and having values of K_{+1} differing by 1, i.e., the pair of energy levels l_{10} and l_{11} .

^{2.} This is a b-type connection and since $\boldsymbol{\mu}_{b}$ is zero it is not allowed.

effects, and the rotational constants which were obtained from fitting the spectra are assumed, the second-order perturbation theory calculation in EIGVALS predicts that at 1 kV electrical potential the |M|=1 component of the 2_{02} - 3_{03} transition should be displaced to higher frequency by 0.5 MHz. The actual displacement is approximately 6 MHz. Furthermore, a plot of Δv vs. ε^2 for this component shows an upward curvature; i.e., $\partial v/\partial \varepsilon^2$ increases with increasing ε .

Since the dipole moment components are accurately known, the origin of the discrepancy in the $|\mathbf{M}|=1$ component of the 2_{02} - 3_{03} transition must lie in the value of the A rotational constant. Calculation of the Stark shift of this transition by direct diagonalization of the entire energy matrix for a variety of values of A gave good agreement with experiment for a range of values of A between two distinct values. The upper bound occurs as A is increased to approximately 15066.MHz where the energy of the 2_{02} level becomes less than that of the 1_{11} level. (1) This causes a change in sign of the Stark contribution from the 2_{02} - 1_{11} connection which results in a change in sign of the calculated displacement. The lower bound results when A is decreased to approximately 14946.MHz where the energy of the 2_{02} level becomes greater than that of the 1_{10} level. This results in a sign change of this connection and an abrupt increase of more than two orders of magnitude in the calculated slope. The region of best agreement occurs at A = 15050.+ 15. MHz.

4.5 Discussion of Results

There are three important results of this study. First, the configuration with the vinyl group trans to the ring is confirmed to

^{1.} The energy of the 1_{10} and 1_{11} levels, given by A + C and A + B respectively, depend strongly on A. By contrast the energy of the 2_{02} level is essentially independent of A.

be the major species present. The evidence supporting this is as follows: the μ_b component of the dipole moment is zero within experimental error, and the experimental rotation constants are in excellent agreement with those calculated assuming a trans configuration. This result is not surprising in view of the fact that there is a close approach of hydrogen atoms in either the gauche or the cis configuration. Also, in the cis configuration CH bonds would eclipse one another across the ${\rm C_1C_5}$ bond. However, previous results on cyclopropylcarboxaldehyde, cyclopropane carboxylic acid fluoride, cyclopropyl methyl ketone, and cyclopropane carboxylic acid chloride show that eclipsed CH bonds across a bond to the cyclopropyl ring are by no means unusual. This geometry has been rationalized previously as being due to the apparent ability of the cyclopropane ring to conjugate with attached π -bond systems.

The second result concerns information about the nature of the torsional potential about the CC bond joining the vinyl group to the ring. Unfortunately it was not possible to assign transitions to a second species. Thus, the conclusion of Lüttke and de Meijere that the second species is a gauche conformer whose population is one-third that of the trans species at 20° C (\triangle G = 1.1 kcal/mole) could not be confirmed.

Also, the kind of analysis performed by Volltrauer and Schwendeman could not be carried out. The apparent absence of spectra due to a second species may be rationalized on one or more of the following grounds: (1) the population may be less than the 12% at -78°C predicted by the Lüttke-de Meijere value of ΔG , i.e., the Lüttke-de Meijere ΔG may be too small; (2) the dipole moment of the second species may be considerably smaller than that of the trans species thereby making the intensity ratio considerably smaller than the population ratio; or (3) there may be a severe vibration-rotation interaction in the second

species which could make it very difficult to assign the transitions. However, even without a second species the fact that transitions in five excited states of the torsional motion have been observed and that the frequencies of the transitions vary linearly with the vibrational quantum number restricts the shape of the potential function and also implies that the barrier to conversion to a second species must be of the order of 3 kcal/mole or higher.

The third result of this study is the value of the dipole moment shown in Table 8. Comparison of this value with those of other hydrocarbons (Table 9) shows that the dipole moment of trans-vinylcyclo-propane is unusually high. The well-known comparison of a cyclopropane ring to a vinyl group would suggest that there would be considerable cancellation of dipole moment contributions in this molecule and that the dipole moment would be unusually small rather than so large.

V. MOLECULAR ROTATIONAL RESONANCE SPECTRUM OF METHYLDIFLUOROPHOSPHINE

5.1 Introduction

A study of methyldifluorophosphine was undertaken as a result of the recent interest expressed in difluorophosphine derivatives in these laboratories and elsewhere (50-54). Determination of the barrier to internal rotation would provide an interesting comparison to the reported values for methylphosphine (55), methylamine (56), methyldifluoroamine (57), and methyldifluoroarsine (58) of 1959, 1980, 4170 and 1325 cal/mole, respectively. The barrier for methyldifluoroamine has been discussed by Pierce, et al. (57) in terms of the CXF or CXH angle. The marked decrease in the barrier for methyldifluoroarsine is almost certainly due to steric interactions since structural calculations using the reported molecular parameters indicate the H-F distance is less than the sum of the Van der Waals radii.

Any forthcoming structural information could be compared to the reported P-C bond lengths for methylphosphine (55) and cyanodifluorophosphine (52) and the FPF and CPF angles to those reported in (50-54).

The sample of methyldifluorophosphine was obtained from Dr. K. Cohn and was used without further purification. The rotational spectrum was observed at both room and Dry Ice temperatures.

5.2 Rotational Constants

The preliminary principal moments of inertia and rotational constants were calculated from the assumed molecular parameters given

in Table 10. The resulting atomic coordinates in the principal axis system and rotational constants are given in Table 11. The projection of the molecule onto the molecular plane of symmetry (the a-c inertial plane) is shown in Figure IV. Since the b axis is perpendicular to the plane of symmetry, the b component of the dipole moment, μ_{b} , should be zero; therefore only a and c-type transitions should be observed. The preliminary rotational constants indicate that methyldifluorophosphine is a near oblate symmetric top (A approximately equals B and both are larger than C). The rotational constants were used with the computer program EIGVALS to calculate approximate rotational energy levels and transition frequencies, as previously described.

An initial search in the predicted spectral regions disclosed the 0_{00} - 1_{01} and 1_{11} - 2_{12} transitions which were identified by their characteristic Stark effect. Since the frequencies of these transitions are given by the expressions (B + C) and (B + 3C), respectively, the B and C rotational constants could be determined. Observation of the 1_{10} - 2_{11} transition, whose frequency is given by (3B + C), confirmed this partial assignment. The assignment was completed by the observation of the 1_{01} - 2_{02} and 1_{01} - 2_{20} transitions which depend strongly on the value of the A rotational constant. The assignment was confirmed by the observation of two R-branch, a-type J = 2 - 3 transitions and several Q-branch a-type transitions.

The Q-branch transition frequencies are given by (59) as,

$$v = 1/2(A-C)\Delta E(\kappa)$$

where $E(\kappa)$ is a dimensionless parameter called the reduced energy and $\Delta E(\kappa)$ is the difference between the values of $E(\kappa)$ for the upper and lower energy states. The reduced energy $E(\kappa)$ is a function of the asymmetry parameter κ defined by $\kappa = (2B-A-C)/(A-C)$ and has been

Table 10. Assumed Molecular Parameters for Methyldifluorophosphine.

r(PF)	1.57 Å	<(FPF)	97°
r(PC)	1.84	<(FPC)	101°
r(CH)	1.093	<(PCH)	109°

Table 11. Atomic Coordinates and Rotational Constants of Methyldifluorophosphine in the Principal Axis System.^a

Atom	a	b	С
P	0.025 Å	0.000 Å	-0.523 Å
F ₁	0.653	1.176	0.307
F ₂	0.653	-1.176	0.307
С	-1.636	0.000	0.269
н	-1.525	0.000	1.356
H ₂	-2.189	0.891	-0.037
Н ₃	-2.189	-0.891	-0.037
	A = 733	3. MHz	
	B = 673	0.	
	C = 441	5.	

a The molecular parameters in Table 10 were assumed.

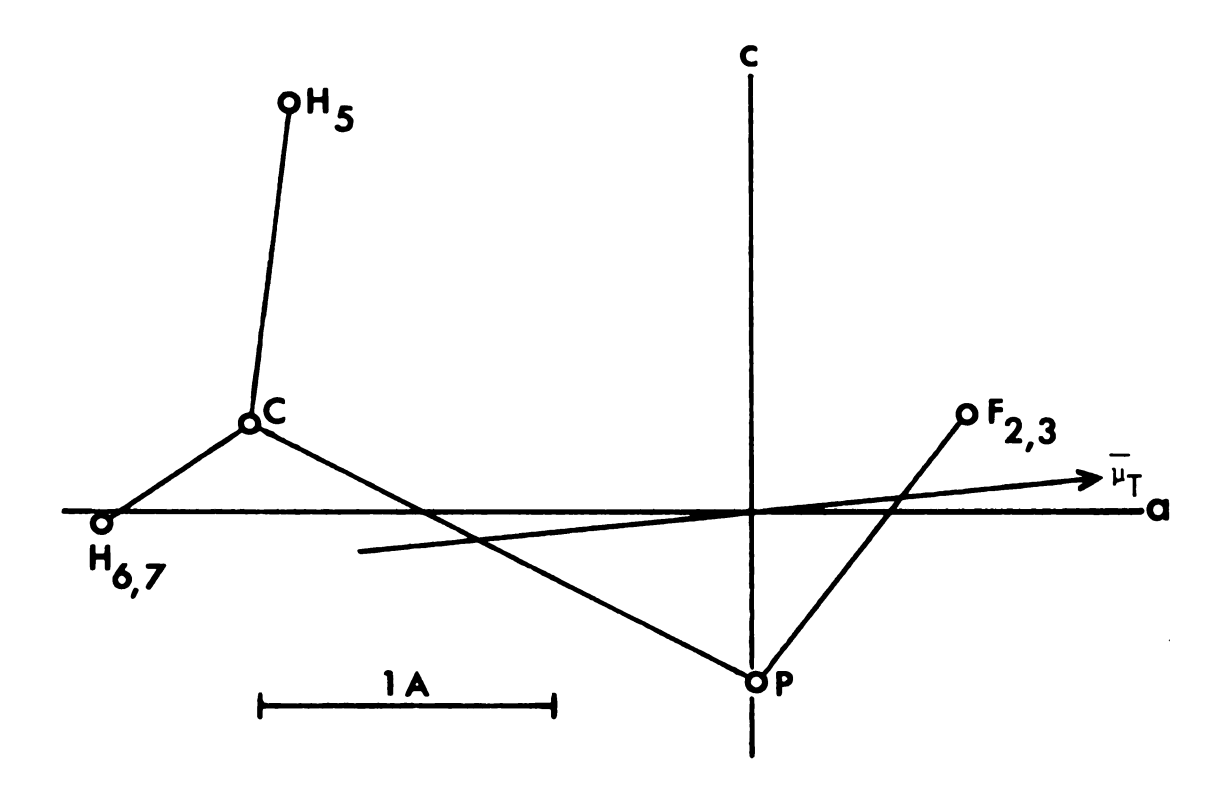


Figure IV. Projection of methyldifluorophosphine onto the molecular symmetry plane. The orientation of the dipole moment vector, $\boldsymbol{\mu}_T$, is also shown.

extensively tabulated (60). Plots of $v/\Delta E(\kappa)$ <u>vs.</u> κ for the various Q-branch transitions should all intersect at a common point, thereby defining the correct values of 1/2(A-C) and κ . This method is very useful in cases where either A or C is not well determined and Q-branch transitions are observed. Plots for several members of the Q-branch series $J_{J-2,3} + J_{J-2,2}$ are shown in Figure V. The graphical value for 1/2(A-C) of 1395.5 MHz is in excellent agreement with the value of 1395.40 MHz obtained by least-squares fitting of the frequencies.

The assigned transitions and their observed frequencies are given in Table 12. The rotational constants were determined by a least squares analysis of the first seven transitions listed in Table 12 and are given in Table 13.

A search for vibrationally excited states revealed that each R-branch transition is accompanied at lower frequencies, and each Q-branch transition is accompanied at higher frequencies, by a much weaker transition which exhibits a Stark effect identical to that of the main transition, as expected for vibrationally excited states. These transitions were assigned to the first excited torsional state, v = 1, of the methyl group about the P-C bond. The assigned transitions and their observed frequencies are given in Table 12 and the rotational constants derived from the five R-branch transitions are given in Table 13. Plots of $v/\Delta E(\kappa)$ vs. κ for the three Q-branch transitions are shown in Figure VI and the graphical value of 1413.8 MHz for $v/\Delta E(\kappa)$ agrees well with the fitted value of 1413.87 MHz.

5.3 Molecular Structure

Since no isotopic species were studied for methyldifluorophosphine, it is impossible to obtain the molecular structure unless assumptions

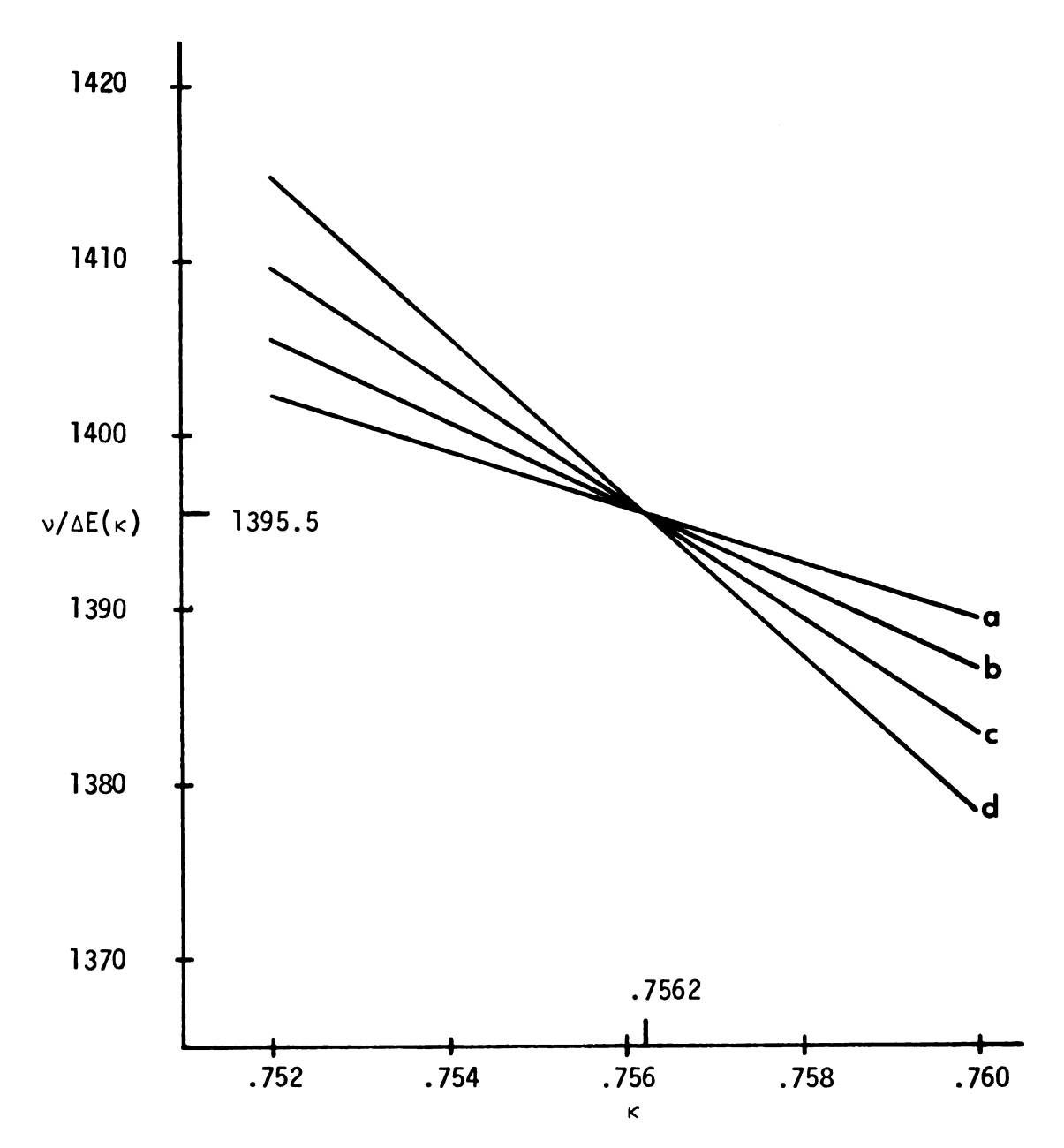


Figure V. Plots of $v/\Delta E(\kappa)$ vs. κ for the a) 6_{43} - 6_{42} , b) 7_{53} - 7_{52} , c) 8_{63} - 8_{62} and d) 9_{73} - 9_{72} Q-branch transitions of methyldifluorophosphine.

Table 12. Comparison of Observed and Calculated^a Frequencies^b for the Ground and First Excited Torsional State of Methyldifluorophosphine.

Transition	v = 0	v = 1
⁰ 00 ⁻¹ 01	11179.90(9.79)	· · · · · · · · · · · · · · · · · · ·
¹ 01 ⁻² 02	20216.04(5.97)	20154.51(4.44)
¹ 01 ⁻² 20	30765.04(4.81)	
¹ 11 ⁻² 12	19908.95(8.87)	19839.71(9.73)
¹ 10 ⁻² 11	24810.36(0.29)	24797.17(7.16)
² 12 ⁻³ 13	28788.33(8.29)	28674.26(4.27)
² 11 ⁻³ 12	34396.54(6.68)	34355.29(5.28)
² 21 ⁻³ 22	33539.24(9.37)	
² 02 ⁻² 21	8405.39(5.40)	
³ 13 ⁻³ 12	12960.52(0.53)	
3 ₀₃ -3 ₂₂	13125.39(5.50)	
⁴ 22 ⁻⁴ 41	10092.18(2.74)	
⁴ 13 ⁻⁴ 32	13223.01(3.60)	
⁴ 23 ⁻⁴ 22	12733.52(3.92)	
⁵ 33 ⁻⁵ 32	12317.97(8.70)	
⁵ 32 ⁻⁵ 51	11575.81(6.86)	
6 ₃₄ -6 ₃₃	18085.57(7.65)	
6 ₄₃ -6 ₄₂	11680.69(1.74)	
7 ₅₃ - ₅₂	10822.73(4.03)	10906.70(8.66)
8 ₆₃ -8 ₆₂	9772.44(3.88)	9826.54(8.95)
9 ₇₃ -9 ₇₂	8574.28(5.70)	8597.59(600.28)

a Last three digits of calculated frequencies are in parenthesis.

b In MHz. Measured frequencies are ±0.05 MHz.

Table 13. Rotational Constants^a, Principal and Second Moments of Inertia^b for the Ground and First Excited Torsional State of Methyldifluorophosphine.

	$\mathbf{v} = 0$	v = 1
Α	7155.34	7167.99
3	6815.25	6818.96
	4364.54	4340.25
I a	70.6292	70.5045
I _b	74.1537	74.1133
I _c	115.7913	116.4392
aa	59.6579	60.0240
bb	56.1334	56.4152
cc	14.4958	14.0893

a In MHz. Uncertainties are as follows: A, \pm .05 MHz; B, \pm .05 MHz; C, \pm .05 MHz.

b In $u \cdot \mathring{A}^2$. Assumed conversion factor of 505376 $\cdot (u \cdot \mathring{A}^2)$ (MHz).

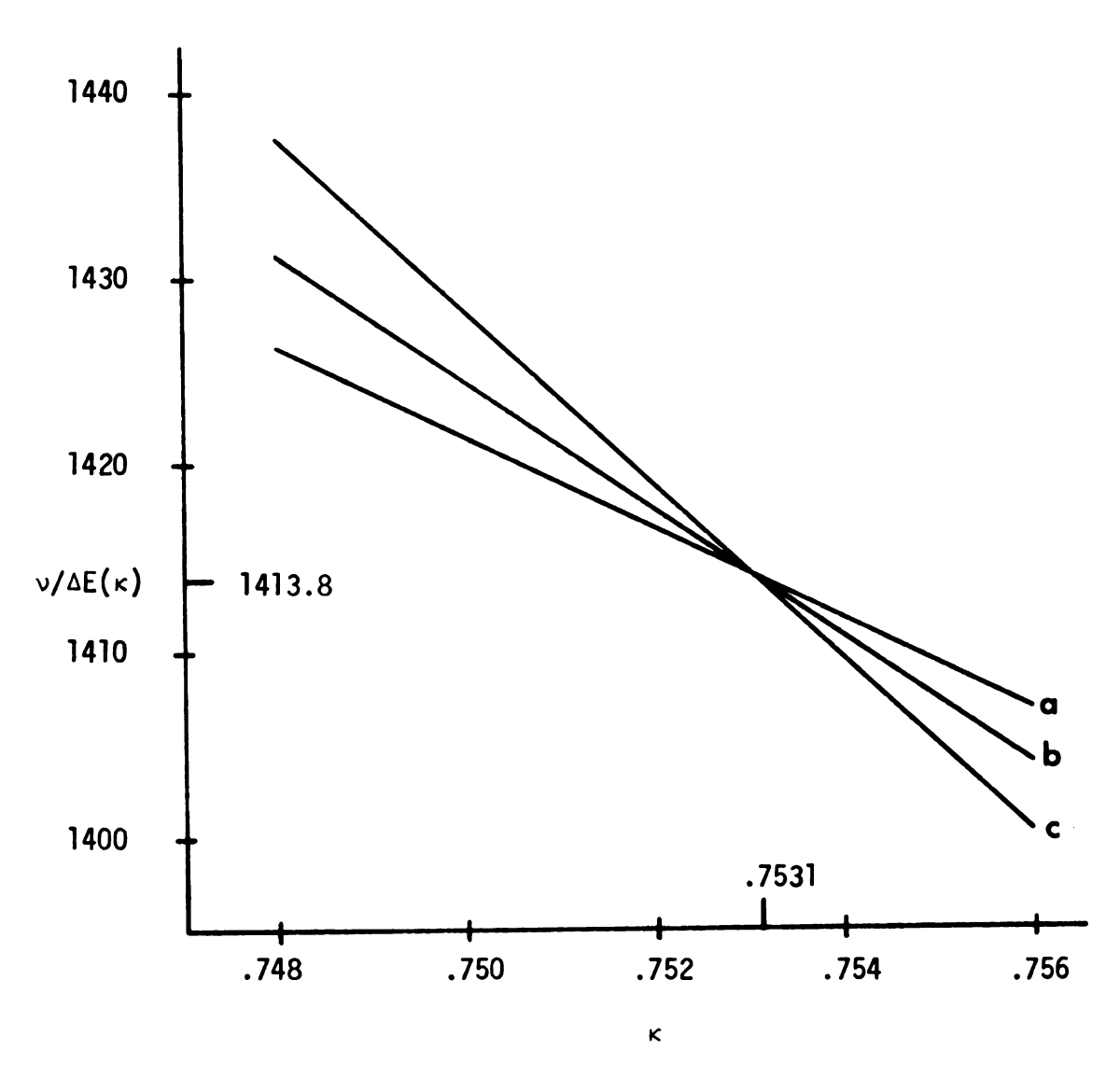


Figure VI. Plots of $v/\Delta E(\kappa)$ vs. κ for a) 7_{53} - 7_{52} , b) 8_{63} - 8_{62} and c) 9_{73} - 9_{72} of the first excited torsional state of methyldifluorophosphine.

are made concerning some of the molecular parameters. There is ample evidence available to support the assumption that the geometry of a methyl group is relatively insensitive to its environment and that reasonable parameters for its geometry could be taken as; r(CH), 1.093 Å and <(PCH), 109.7° . If the PF bond length is also assumed, the remaining molecular parameters, r(PC), <(FPF) and <(FPC), may be determined by a fit of the rotational parameters M_a , M_c , P_{ac} , P_{aa} , P_{bb} , and P_{cc} of the parent species (M_g is the g^{th} center of mass condition defined as $M_g = \sum_{i=1}^{m} g_i = 0$). However it was found, as shown in Table 14, that $g = \sum_{i=1}^{m} g_i = 0$. However it was found, as shown in Table 14, that the calculated PC bond length is quite sensitive to the assumed PF bond length while the FPF and FPC angles are relatively insensitive. Variation of the methyl geometry produces negligible change in the calculated parameters.

Results of some recent structural studies on difluorophosphine derivatives are shown in Table 15. These results indicate that for substituents which have chemical properties and electronegativities similar to those of a methyl group a PF bond length of 1.580 to 1.586 Å is expected. Within this interval the calculated PC bond length is approximately 1.82 Å which lies between the reported values of 1.810 Å and 1.863 Å for cyanodifluorophosphine and methylphosphine (55), respectively.

5.4 The Barrier to Internal Rotation

As previously discussed in Section 2.3, if the potential barrier hindering the internal rotation of the methyl group is low enough, the rotational transitions may be split into doublets consisting of transitions among A and E levels. This splitting is a result of the

Table 14. The PC Bond Length^a, FPF and FPC Bond Angles^b as a Function of the PF Bond Length in Methyldifluorophosphine.

r(PF)	r(PC)	<(FPF)	<(FPC)
1.574	1.842	99.1	97.3
1.576	1.838	98.9	97.4
1.578	1.834	98.8	97.5
1.580	1.829	98.6	97.6
1.582	1.825	98.4	97.8
1.584	1.820	98.3	97.9
1.586	1.816	98.1	97.9
1.588	1.812	97.9	98.1
	Assuming: r(CH) = 1.093 Å	
	(HC	H) = 109.2°	

a In Angstroms.

Table 15. Molecular Parameters for Some Difluorophosphine Derivatives.

Molecule	r(PF)	< (FPF)	< (FPX)	Ref.
PF ₂ 0CH ₃	1.586 Å	95.3°	101.5°	this work
PF2NH2	1.586 Å	94.7°	101.7°	50
PF ₂ H	1.582 Å	99.0°	96.3°	54
PF ₂ C1	1.571 Å	97.3°	99.2°	51
PF ₂ CN	1.567 Å	99.1°	97.2°	52

b In degrees.

coupling of the internal and overall angular momenta. The magnitude of the splitting may be used to evaluate the barrier height.

Careful examination of the spectrum for methyldifluorophosphine failed to disclose any splittings in either the ground or first excited torsional states. Assuming that any splitting greater than 0.5 MHz could be resolved, theoretical calculations were performed on the first excited state in an attempt to establish a lower bound to the barrier. Results of these calculations indicate that the barrier to internal rotation in methyldifluorophosphine must be at least 3600 ± 200 cal/mole.

The height of the potential barrier may also be determined from the torsional excitation energy. If the excitation energy is large, the potential function hindering the torsion will be essentially harmonic and α , the torsional angle, will be small. With these assumptions the expression for a threefold barrier may be written as;

$$V_3 = 8\pi^2 c^2 v_T^2 I_r/9$$

where v_T is the torsional excitation energy in cm⁻¹ and I_r is the reduced moment of interia of the internal rotor about its symmetry axis. I_r is defined as (11),

$$I_{r} = I_{\alpha}[1-I_{\alpha}\sum_{q=1}^{\lambda_{q}}] \quad g = a, b, c$$

where λ_g is the direction cosine between the g^{th} principal axis and the symmetry axis of the internal rotor and I_g is the g^{th} principal moment of inertia.

The value of $\boldsymbol{\nu}_{T}$ may be estimated from relative intensity data as;

$$v_T = KTln(I_{v=1}/I_{v=0})$$

where the I's are the relative intensities of the same rotational transitions

in the ground and first excited torsional states. The intensities were measured at room temperature using the Hewlett-Packard model 8460 A R-band spectrometer. Unfortunately, it proved impossible to locate any ground state - first excited state pairs which were completely free from interference due to overlapping transitions or Stark lobes from adjacent transitions. However, the results of twenty-one measurements on the 2_{11}^{-3} transitions (the most satisfactory pair) gives an average value of 318 ± 30 cm⁻¹ for the excitation energy. To confirm this value an infrared spectrum was taken in the region 250-400 cm⁻¹; the corresponding absorption was observed at 325 ± 15 cm⁻¹. Since this value must be more reliable than the relative intensity value, it was used with the above equation to calculate a value for the barrier height of 6.1 ± 0.3 kcal/mole. The indicated uncertainty is greater than that resulting from v_T due to the uncertainty in I_r from the assumed structure.

Pierce, et al. (57) have discussed the large increase in the barrier of CH_3NF_2 (4170 cal/mole) compared to CH_3NH_2 (1980 cal/mole) in terms of the CNX angle. They point out that the CNF angle in CH_3NF_2 is some 7.4° smaller than the CNH angle in CH_3NH_2 . Additional evidence is supplied by the comparison of CH_3SH (1270 cal/mole) with CH_3OH (1070 cal/mole) where the CSH angle is 6.5° smaller than the COH angle. Indeed, it does seem intuitively reasonable to expect the barrier to increase as this angle decreases. However, comparisons of CH_3OH to CH_3OCl (3060 cal/mole), where the COCl angle is 7° larger than the COH angle, and CH_3PF_2 to CH_3PH_2 , where the CPX angles are essentially equal, serve to point out that such simple approaches are not entirely reliable.

5.5 Dipole Moment

Displacements of the Stark components as a function of the electric field were determined for the M = 0 components of the J = 0 \rightarrow 1 and the three J = 1 \rightarrow 2 transitions. The resulting slopes, $\frac{\partial \nu}{\partial \varepsilon}$ 2, were used with Eq. (2-16) to calculate the three dipole moment components. As expected, the b component, μ_b , was zero within experimental error. With μ_b set equal to zero the a and c components were then recalculated. The observed and calculated slopes along with the resulting dipole moment components and total dipole moment are given in Table 16. The total dipole moment was found to make an angle of 5.5 \pm 0.1° with the a-axis. Although the sign of this angle and the dipole moment itself are not determined by the data, the orientation is most likely that shown in Figure IV.

A comparison of the reported dipole moments for some difluorophosphine derivatives is given in Table 17.

5.6 The Anomalous Stark Effect of the |M| = 1 Component of the 1_{01} - 2_{02} Transition

As previously discussed, when one or more of the energy differences in the denominator of Eq. (2-15) becomes small, the necessary conditions for a second order perturbation treatment are no longer met and a direct calculation is required.

In the present case the 2_{02} and 2_{12} levels are nearly degenerate with the 2_{12} being higher in energy by only 33 MHz. For |M| = 1 a direct c-type connection exists between these levels resulting in a strong perturbation of the Stark energies.

It should be noted that the |M| = 1 component of the $l_{11}-2_{12}$ transition also exhibits an anomalous Stark effect; however, it is

Table 16. The Stark Effect and Dipole Moment of Methyldifluorophosphine.

Transition	$\partial v/\partial \varepsilon^2$) obs	^{aν/aε²)calc}
$0_{00}^{-1}_{01} M = 0$	233.78	233.83
$1_{01}-2_{02}$ M = 0	60.88	60.80
$1_{11}-2_{12} M = 0$	-73.38	-73.26
1 ₁₀ -2 ₁₁ M = 0	48.05	48.13
	$\mu_a = 2.047 \pm 0.002 D$	
	μ_{b} = 0.0 D	
	$\mu_{C} = 0.194 \pm 0.03 D$	
	μ _T = 2.056±0.03 D	

a Hz/(volt/cm)² assuming μ_{OCS} = 0.7152 D.

b Uncertainty in observed slopes is ±0.5%.

Table 17. Comparison of the Dipole Moments^a for Some Phosphine and Difluorophosphine Derivatives.

Compound	μ <mark>α</mark> Τ	Ref.
Methylphosphine	1.100	55
Difluorophosphine	1.32	54
Cyanodifluorophosphine	2.393	52
Aminodifluorophosphine	3.029	50
Chlorodifluorophosphine	0.89	51
Methyldifluorophosphine	2.056	This study

a In Debyes.

somewhat less spectacular than that of the 1_{01} - 2_{02} transition illustrated here.

The observed Stark effect is as follows: as the applied voltage is increased the Stark component is displaced to lower frequency until it reaches a maximum displacement of approximately -4.8 MHz at 375 volts. As the voltage is increased further, the component reverses direction and begins to move back toward the zero-field line reaching its original position at approximately 560 volts. Further increase of the applied voltage displaces the component to higher frequency in a nearly normal manner.

With the rotational constants from Table 13 and the dipole moment components from Table 14 a direct calculation was performed by means of the procedure outlined in Section 4.4. The observed and calculated Stark effects are shown in Figure VII. The agreement is excellent, which confirms the calculated values of the dipole moment components.

5.7 Discussion of Results

There are three important results of this study, the PC bond length, the barrier to internal rotation of the methyl group, and the dipole moment.

To determine the PC bond length from only three moments of inertia it was necessary to make several assumptions. The values assumed for the CH bond distance, PCH bond angle, and tilt of the methyl group all had relatively slight effects on the remaining parameters. One more assumption was necessary and the PF bond distance was selected. Recent determination of PF bond distances in PF_2X molecules demonstrates a dependence of the PF distance on the electronegativity of the group X (Table 15). Values for this distance near the value in PF_2H were

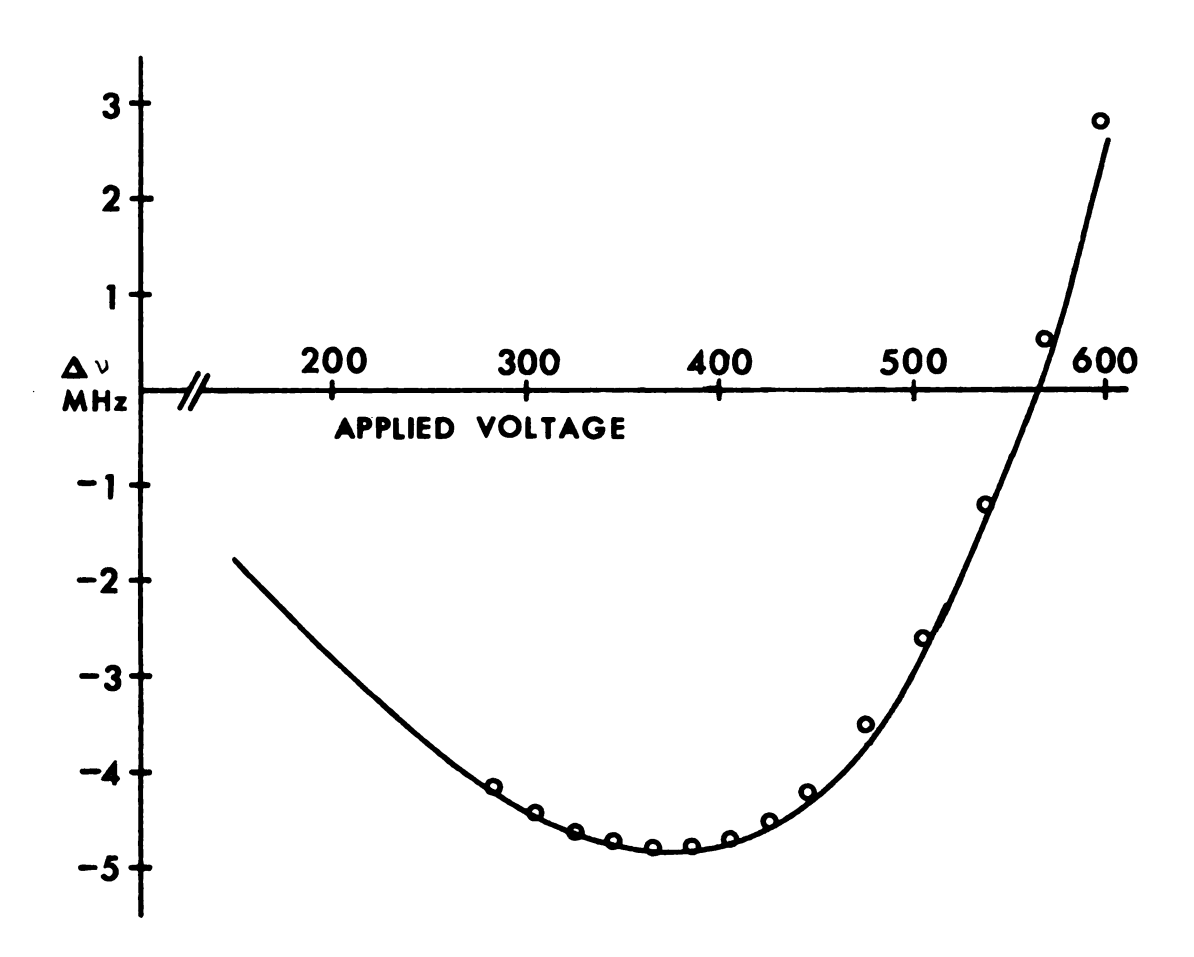


Figure VII. Comparison of the observed (circles) and calculated (solid line) Stark effect for the |M|=1 component of the 1_{01} - 2_{02} transition.



selected and the remaining parameters were determined as described above (Table 14). The best value of the PC bond distance appears to be near 1.82~Å which is 0.04~Å shorter than the value reported for CH_3PH_2 . This is a significant difference in an important bond length and should be verified by studies of the ^{13}C species in the molecules.

The barrier to internal rotation, 6.1 kcal/mole, determined here from the torsional splittings is larger than the barrier in CH_3NF_2 (4.17 kcal/mole) and considerably larger than in CH_3AsF_2 (1.325 kcal/mole). As mentioned above, the barrier height in CH_3NF_2 has been discussed by Pierce et al. (57) in terms of the CNF angle. A similar reasoning does not seem valid here since the bond angles in CH_3PF_2 and CH_3PH_2 are apparently quite similar.

The dipole moment in CH_3PF_2 (2.056 D) is considerably larger than that in PF_2H (1.32 D). Since the primary electronic effects of CH_3 and H are usually considered to be comparable, this is further evidence of some unusual electronic effect in CH_3PF_2 .

VI. MOLECULAR ROTATIONAL RESONANCE SPECTRUM OF METHOXYDIFLUOROPHOSPHINE

6.1 Introduction

The study of methoxydifluorophosphine was undertaken as a result of the recent interest in difluorophosphine derivatives as mentioned above.

Methoxydifluorophosphine appeared to be an excellent example for further investigation of the effects of $(p-d)\pi$ bonding resulting from the delocalization of the oxygen p-orbital lone pairs into the vacant d-orbitals on phosphorus. Bonding of this type has been recently postulated to account for the planarity of the -NH $_2$ group in NH $_2$ PF $_2$. To determine the structure of the molecule the MRR spectra of the parent compound and three isotopically labeled species were investigated. In addition, it was expected that the structural data would provide additional information regarding the relationship of the PF $_2$ geometry to the electronegativity of the substituent and also determine the molecular configuration.

Because of the moderate barrier height characteristically associated with internal rotation about a C-O bond, as shown in Table 18, the rotational transitions should be split into doublets due to coupling with this motion. Analysis of the splittings would yield the height of the potential barrier to internal rotation.

Table 18. Barriers to Internal Rotation of Methyl Groups About the C-O Bonds.

Compound	Formula	V ₃ (cal/mole)	Ref.
Methanol	сн ₃ он	1070.	62
Methyl formate	сн ₃ соон	1190.	63
Methyl nitrate	CH ₃ 0NO ₂	2321.	64
Dimethyl ether	(CH ₃) ₂ 0	2720.	65
Ethylmethyl ether	C ₂ H ₅ OCH ₃	2530.	66

6.2 Preparation of Samples

The normal and isotopic species of methoxydifluorophosphine were prepared in collaboration with Dr. C. E. Jones (1) by the following reactions:

$$\begin{array}{c} \text{CH}_3\text{OH} + \text{PCl}_3 \rightarrow \text{CH}_3\text{OPCl}_2 + (\text{CH}_3\text{O})_2\text{PCl} + \text{HCl+} + \text{PCl}_3 \\ \\ \underline{\text{upon}} \\ \text{standing} \rightarrow \text{CH}_3\text{OPCl}_2 \\ \\ \text{CH}_3\text{OPCl}_2 + \text{SbF}_3 \xrightarrow{\text{SbCl}_5} \text{CH}_3\text{OPF}_2 \end{array}$$

The experimental details are as follows: 0.5 g (0.016 moles) of methanol is added dropwise with stirring to 2.33 g (0.017 moles) of phosphorus trichloride in a small round bottom flask. The reaction is slightly exothermic and hydrogen chloride gas is evolved. A mixture of products, consisting of methoxydichlorophosphine and dimethoxychlorophosphine is initially formed; however, upon standing dimethoxychlorophosphine further reacts with the excess phosphorus trichloride to give a near quantitative yield of methoxydichlorophosphine. This conversion is conveniently monitored by periodically examining the proton NMR spectrum which consists of two overlaping doublets. One doublet, due to methoxydichlorophosphine, is centered at a chemical shift of 3.8 ppm with a coupling constant, J_{P-H} , of 10 Hz. The other doublet, due to dimethoxychlorophosphine, is centered at 3.7 ppm with a coupling constant of 13 Hz. The reaction mixture is allowed to stand until the integrated proton NMR spectrum indicated that the reaction was approximately 95% complete, which usually took 12-16 hours.

The methoxydichlorophosphine sample is fluorinated by slowly dropping it onto solid, finely ground antimony trifluoride which has been

^{1.} Present address: University of Leeds, Leeds, England.

wetted by approximately 5% by weight of antimony pentachloride which acts as a catalyst. The gaseous products are collected in a trap at -78°C. The products are partially separated by trap-to-trap distillation with traps at -78°C, -112°C and -196°C. The fraction collected at -112°C is retained. Final purification is accomplished by low-temperature co-distillation using helium as the carrier gas.

The isotopic species were prepared in the same manner starting with 60% $^{13}\text{CH}_3\text{OH}$, 40% CD₃OH, and 40% CH₃ ^{18}OH .

6.2 Rotational Constants

Since the barrier to internal rotation of a methyl group about a C-O bond is typically of moderate height (Table 18), the rotational transitions were predicted to appear as doublets due to the internal rotation splitting (see Section 2.3). If the barrier is not too low, the A-level transitions should still closely approximate the rigid-rotor model and, barring any accidental degeneracies, exhibit the normal second order Stark effect. However, the E-levels may not fit the rigid-rotor approximation since the internal rotation introduces terms containing odd powers of the angular momenta. Furthermore, since the E-levels are doubly degenerate ($\sigma = \pm 1$) the E-level transitions may exhibit a first-order Stark effect and thus be readily discernible from the A-levels.

After selecting representative molecular parameters from similar compounds, the computer programs STRUCT and EIGVALS were used to calculate the preliminary rotational constants, rotational energy levels and transition frequencies. A plane of symmetry was assumed with the carbon atom cis to the fluorine atoms, as shown in Figure VIII. The calculations predicted that the molecule should be a near prolate top

with the b axis perpendicular to the molecular plane, and therefore that a and c-type transitions should be observed.

Initial examination of the spectral regions predicted for the J = 4-5 and J = 5-6 a-type transitions of the normal species and analysis of the Stark effects of the prominent transitions in these regions confirmed the presence of A and E level doublets split by internal rotation. The A-level, a-type J = 4.5 and J = 5.6 transitions were assigned by their characteristic Stark effects and their positions relative to one another. Only the two lowest energy J = 5.6 transitions were observed; the remaining transitions occur at frequencies which are higher than those presently attainable in these laboratories. Since methoxydifluorophosphine is approximately a near prolate top the a-type transitions are not strongly dependent upon the A rotational constant. Therefore an effort was made to selectively assign those transitions with the greatest dependence upon the A rotational constant rather than to assign and measure the frequencies of all the available transitions. The observed and calculated frequencies of the assigned transitions for the A-levels of the normal species are given in Table 19. The rotational constants, principal and second moments of inertia derived from these frequencies are given in Table 21.

Initial values of the rotational constants for the isotopic species were obtained by adding the difference between the STRUCT and experimental rotational constants of the normal species to those calculated by STRUCT for the isotopic species. These rotational constants were then used with EIGVALS to calculate the approximate rotational energy levels and transition frequencies. In this manner it was possible to predict the experimental transition frequencies to within +15 MHz, thus making assignment of the spectra quite straightforward. An effort was again

Table 19. Comparison of Observed and Calculated^a Frequencies^b and Internal Rotation Splittings for ${\rm CH_30PF_2}$ and ${\rm ^{13}CH_30PF_2}$.

	CH ₃ 0PF ₂)F ₂	13CH30PF2	
Transition	Frequency	Δν(Α-Ε)	Frequency	Δν(A-E)
321-422	27692.99(2.66)		26947.08(6.97)	
322-423	27019.89(9.67)			
312-413			27225.84(5.54)	
414-515	32298.16(7.80)	-316.29(6.75)	31565.68(5.34)	-305.68(5.66)
404-505	32667.54(7.33)	426.08(6.63)	31955.63(5.39)	406.09(5.66)
423-524	33680.87(0.95)			
413-514	34726.94(6.86)	114.44(4.85)	33871.43(1.38)	99.08(9.23)
431-532	34182.60(3.28)			
422-53	34857.83(7.70)		33913.17(3.22)	
515-616	38636.59(6.61)	-282.50(3.02)	37769.26(9.30)	-285.41(5.61)
₅₀₅ -6 ₀₆	38876.41(6.60)	424.50(5.06)	38035.08(5.21)	417.00(6.56)
524-625			39319.32(9.93)	
533-634			39833.73(5.01)	

MHz. a Last three digits of the calculated values are in parenthesis. b In MHz. Measured frequencies are ±0.05

Table 20. Comparison of Observed and Calculated^a Frequencies^b and Internal Rotation Splittings for ${\rm CD_30PF_2}$ and ${\rm CH_3}^{18}{\rm OPF_2}$.

	CD ₃ OPF ₂	PF2	CH3 ¹⁸ 0PF2	
Transition	Frequency	∆∨(A-E)	Frequency	Δν(Α -Ε)
414-515			31833.341(3.06)	-310.258(1.15)
404-505	29695.570(5.19)	23.933(3.95)	32212.326(2.07)	417.375(7.34)
413-514			34115.975(5.79)	105.479(6.02)
⁴ 22 ⁻⁵ 23	31172.395(2.13)	10.243(0.31)	34171.794(1.70)	
919-919	35068.898(8.91)	-11.587(1.68)	38090.630(0.68)	-285.711(6.59)
₅ 05 ⁻⁶ 06	35367.476(7.57)	40.472(0.61)	38346.714(6.85)	424.978(4.80)
524-625	36375.384(5.71)	5.143(5.21)	39627.359 (7.85)	
523-624	37584.339(4.43)	5.612(5.69)		

a Last three digits of the calculated values are in parenthesis.

b In MHz. Measured frequencies are ± 0.05 MHz.

Table 21. A Level Rotational Constants^a, Principal and Second

Moments of Inertia^b for the Normal and Three Isotopic

Species of Methoxydifluorophosphine.

	CH ₃ OPF ₂	13 _{CH3} OPF ₂	сн ₃ 180РF ₂	CD ₃ OPF ₂
1	5991.04	5973.28	5935.14	5718.40
	3641.81	3542.67	3566.40	3252.63
	3127.85	3058.98	3086.88	2894.59
	84.35529	84.6062	85.1480	88.3771
	138.77038	142.6538	141.7050	155.3745
	161.77038	165.2107	163.7173	177.6618
a	107.99387	111.6292	110.1363	122.3296
b	53.57878	53.5815	53.5811	55.3322
С	30.77651	31.0246	31.5687	33.0449

a In MHz. Uncertainties are as follows: A, ± 0.1 MHz; B, ± 0.05 MHz; C, ± 0.05 MHz.

b In $u \cdot \mathring{A}^2$. Assumed conversion factor of 505376. $(u \cdot \mathring{A}^2)(MHz)$.

made to selectively assign and measure the frequencies of those transitions having the greatest dependence on the A rotational constant. The assigned transitions and observed frequencies for the isotopic species are given in Tables 19 and 20, while the calculated values of the rotational constants, principal and second moments of inertia are given in Table 21.

6.4 Barrier to Internal Rotation

The low potential barrier hindering the internal rotation of the methyl group resulted in large splittings between the A and E levels. To account for these splittings terms to fourth order were included in the calculation of the $H_{V\sigma}$ matrix of Eq. (2-11),

$$H_{V_{\sigma}} = H_{r} + F_{n=1}^{2} W_{V_{\sigma}}(n)_{p}n$$

The matrix elements which are required for $H_{V\sigma}$ have been given by Herschbach (11). The resulting energy matrix, which factors into blocks of order 2J + 1 for each J, was diagonalized; the eigenvalues are the desired energy levels. The calculations were carried out using a computer program, INROT, which was written for use on the Control Data 6500 computer.

As mentioned previously, the transitions among E-levels exhibit a first order Stark effect and thus are readily discernable from the A-level transitions. A preliminary internal rotation calculation was made using a barrier height of 1. kcal/mole to predict the frequencies of the E transitions. Once this information was available the E transitions were readily assigned. The assigned E level transitions and the observed internal rotation splittings (ν_{A} - ν_{E}) for the normal and three isotopic species are given in Tables 19 and 20.



The internal rotation parameters, the three-fold barrier height (V_3) , the moment of inertia of the internal rotor about its symmetry axis (I_α) , and the angle between the symmetry axis of the internal rotor and the a principal axis (θ) , were calculated by a least squares fit of the A-E splittings. The molecule was assumed to have a plane of symmetry such that the direction cosine, λ_b , between the symmetry axis of the internal rotor and the out-of-plane b axis was zero. It was further assumed that the A-E splittings would vary linearly with the various parameters q_i as,

$$\delta \Delta v_{\mathbf{j}} = \sum_{\mathbf{i}} \left(\frac{\partial \Delta v_{\mathbf{j}}}{\partial q_{\mathbf{i}}} \right) \delta q_{\mathbf{i}}$$

The derivatives $\partial \Delta v_i/\partial q_i$ where evaluated numerically by changing the q_i 's in small increments and noting the effect on the Δv_i 's. If the resulting values of the q_i 's fell outside the increments used to evaluate the derivatives, the increments were readjusted and the entire process repeated. Although the Δv_j 's are also functions of the rotational constants the derivatives with respect to the rotational constants were found to be very small and therefore these terms were not included in the least squares fit. The parameters were fit without constraints to yield the best agreement to the observed splittings of the normal species. Since ^{13}C or ^{18}O isotopic substitution should not affect either \textbf{V}_{3} or $\textbf{I}\alpha$, these parameters were held constant and only θ was fit for these isotopic species. Deuterium substitution on the methyl rotor not only nearly doubles $I\alpha$ due to the increase in mass but also results in an effective shrinkage of the methyl rotor due to "zero point" vibrational effects (66). Therefore it was necessary to include all three parameters in the least squares fit for the CD_3OPF_2 . The results of these calculations for V_3 , I^{α} and θ are given in Table 22.

Table 22. Internal Rotation Parameters for the Normal and Three Isotopic Species of Methoxydifluorophosphine.

	$c_{\mathrm{H_3}}$ OPF $_2$	13 CH $_3$ OPF $_2$	сн ₃ ¹⁸ 0РF ₂	CD ₃ 0PF ₂
٧3	422. <u>+</u> 5. cal/mole			405. ± 5. cal/mole
Iα	$3.18 \pm 0.07 \text{ u}^{3}$			6.39 ± .07 u·Å ²
θ	50.68°± 0.1°	49.7° ± 0.1°	51.1° ± 0.1°	47.8° ± 0.1°
, a	.63365	.64639	.62796	.67120
، رن	.77362	.76301	.77824	.74127
S	12.0415	12.0416	12.0467	22.6149
Ŀ	163.3600 GHz	163.3592 GHz	163.2894 GHz	83.4786 GHz

The values of the barrier height calculated in this manner are near the lower limit for which the perturbation treatment of Section 2.3 is applicable. To test the validity of this treatment for the present study a calculation was done using a low-barrier approximation in which free-rotor wavefunctions formed the basis set for the torsion of the methyl group (29,67). The results of this calculation agree with those of the perturbation calculation to within the uncertainties of the perturbation results. As a result, the perturbation treatment was used in all subsequent calculations.

The A-level rotational constants in Table 21 contain a contribution from internal rotation. They were obtained by a least squares fit to a rigid-rotator Hamiltonian. To remove the internal rotation contribution and calculate rotational constants, A_0 , B_0 , and C_0 , which are free of the effects of this motion, the following procedure was employed: the frequencies of the A transitions were computed using the INROT program with approximate rotational constants, Q_{INROT} (Q = A, B, or C). The computed frequencies were then fit by means of program EIGVALS to obtain effective rotational constants, Q_{EFF} . The first approximation to the rotational constants Q_0 was then obtained by the following relation

を見いる ゆうれいば ひとい プロなが しては あるかる これの

$$Q_o = Q_A + (Q_{INROT} - Q_{EFF}).$$

The procedure was repeated until $Q_{EFF} = Q_A$, and $Q_O = Q_{INROT}$. The adjustment of the rotational constants produced no significant changes in the calculated A, E splittings. The resulting effective unsplit rotational constants, and the principal and second moments of inertia are given in Table 23.

Effective Rotational Constants, a Principal and Second Moments of Inertiab for the Normal and Three Isotopic Species of Methoxydifluorophosphine. Table 23.

	CH ₃ 0PF ₂	¹³ сн ₃ орғ ₂	сн ₃ ¹⁸ 0РF ₂	CD30PF2
A _o	5979.398	5961.526	5924.371	5715.354
B _o	3641.845	3542.700	3566.437	3252.640
၀ွ	3123.482	3054.908	3082.552	2843.712
I a	84.51954	84.77293	85.30458	88.42427
$^{ m I}_{ m b}$	138.76923	142.65278	141.70333	155.37409
I _C	161.79891	165.43084	163.94727	177.711
g aa	108.02430	111.65535	110.17301	122.33342
P _{bb}	53.77462	53.77549	53.77426	55.38359
Pcc	30.74493	30.99743	31.53032	33.04068

a In MHz. Uncertainties are as follows: A, \pm 0.1 MHz; B, \pm 0.05 MHz; C, \pm 0.05 MHz.

b In u.A². Assumed conversion factor of 505376 $(u.A^2)$ (MHz).

The uncertainty in V_3 depends primarily on the uncertainty in I_{α} and only slightly on the uncertainty θ . Uncertainties of ± 0.1 u·Å² in I_{α} and $\pm 1^{\circ}$ in θ result in uncertainties of ± 15 cal/mole and ± 2 cal/mole, respectively, in V_3 . The absolute error in the experimental values of the splittings are much smaller than the uncertainties in the calculated splittings and thus make a negligible contribution to the uncertainty in V_3 . The larger uncertainties for the parameters of the CD_3OPF_2 species are a result of the fact that the A, E splittings are much smaller in this molecule than in the other species while the absolute uncertainties in the splittings are comparable.

6.5 Molecular Structure

As discussed in Section 2.5, to obtain a complete Kraitchman substitution structure it is necessary to isotopically substitute at each atomic position. Such a complete substitution is impossible for methoxydifluorophosphine since phosphorous and fluorine each have only one stable isotope. However, if it is assumed that methoxydifluorophosphine possesses a plane of symmetry which bisects the FPF angle and one HCH angle, the four isotopic species studied here are sufficient to determine a complete structure provided that one piece of information about the H atom locations is assumed.

As previously discussed, the isotopic species $\mathrm{CH_3OPF_2}$, $\mathrm{^{13}CH_3OPF_2}$, $\mathrm{CH_3^{18}OPF_2}$, and $\mathrm{CD_3OPF_2}$ were studied and the resulting effective rotational parameters are given in Table 23. However, since the $\mathrm{CD_3}$ species involves simultaneous substitution at two nonequivalent hydrogen positions the resulting information is not directly applicable to the structure determination. Nevertheless it may be used to aid in determining the geometry of the methyl group.

The assumption of a molecular plane of symmetry may be justified by comparison of the P_{bb} values, the out-of-plane second moments of inertia, given in Table 23. P_{bb} is defined as $\sum_{i} m_i b_i^2$ (see Section 2.5) and if the b principal axis is perpendicular to the plane of symmetry any isotopic substitution in the plane should leave P_{bb} unchanged ($b_i = 0$). The fact that the observed P_{bb} values for the normal, ^{13}C , and ^{18}O species are essentially equal provides conclusive evidence for a molecular plane of symmetry.

The principal axis coordinates of the oxygen and carbon atoms were determined using the Kraitchman substitution equations and second moments of inertia for the 18 O and 13 C species, respectively. For these calculations the Kraitchman equations are more conveniently expressed as,

$$|a| = \left[\frac{1}{\mu}(P_{aa}'-P_{aa})(1+\frac{P_{bb}'-P_{bb}}{P_{bb}-P_{aa}})(1+\frac{P_{cc}'-P_{cc}}{P_{cc}-P_{aa}})\right]^{1/2}$$

Equations for |b| and |c| may be obtained by cyclic permutation of the subscripts. Since there is a molecular plane of symmetry which results in a near equality of the P_{bb} values, the factor including the difference in P_{bb} values was set equal to one.

The remaining molecular parameters, i.e., the geometry of the ${\rm CH_3}$ and ${\rm PF_2}$ groups, were determined by a least squares fit to ${\rm M_a}$, ${\rm M_C}$, ${\rm P_{ac}}$, ${\rm P_{aa}}$, ${\rm P_{bb}}$, and ${\rm P_{CC}}$ of the normal species. Since the methyl geometry can not be determined directly from the ${\rm CD_3}$ information, a series of calculations were done for various CH bond lengths and OCH angles to determine the methyl geometry which best predicted the observed moments of inertia of the ${\rm CD_3}$ species. The only constraint placed on the methyl geometry was that it be symmetric, i.e., that the HCH angles be equal. The best agreement was found at a CH bond length of 1.090 \pm 0.003 Å and

an OCH angle of $109.5 \pm 0.2^{\circ}$. As expected, the PF₂ geometry was quite insensitive to small variations in the methyl geometry.

Using the principal axis coordinates of the oxygen and carbon atoms the angle between the OC bond and the a axis was calculated to be $53.11 \pm 0.05^{\circ}$. This result may be compared to the value of θ , the angle between the symmetry axis of the methyl rotor and the a axis, determined from the internal rotation analysis (see Table 22) of $50.68 \pm .1^{\circ}$. The inequality of these two angles indicates that the methyl group is "tilted" such that its symmetry axis no longer lies along the OC bond but is 2.43° away from the OC bond. "Tilted" methyl groups are commonly observed in internal rotation studies (55-57). As in all previous studies where the methyl group is attached to an atom having unshared electron pairs, the methyl "tilt" in this study is toward the unshared electron pairs on the oxygen. Without being specific about the forces involved, the "tilt" can be rationalized as resulting in a lowering of "bond-bond repulsions" at the expense of an increase in "bond-unshared pair repulsions".

The structure fitting calculations were repeated with the methyl group "tilted" 2.43° away from the fluorine atoms with no significant changes in any of the molecular parameters except the OCH angles. The atomic coordinates resulting from the structure calculations are given in Table 24. The corresponding bond lengths and angles are given in Table 25 and the projection of the molecule onto the molecular plane of symmetry is shown in Figure VIII.

Although not strictly chemically correct, it may be instructive to compare the results of this study with the results of x-ray crystallographic studies on some phosphorus (V) compounds containing methoxy groups (Table 26). Cruickshank (71), from a comparison of phosphorus (V)

Table 24. Principal Axis Coordinates^{a,b} for Methoxydifluorophosphine.

Atom	a	b	С
P ₁	0.526 <u>+</u> .005	0.000	-0.549 <u>+</u> .003
	0.529 <u>+</u> .004	0.000	-0.548 <u>+</u> .002
F ₂	0.787 <u>+</u> .004	1.172 <u>+</u> .002	0.489 <u>+</u> .002
	0.784 <u>+</u> .003	1.171 <u>+</u> .002	0.489 <u>+</u> .002
F ₃	0.787 <u>+</u> .004	-1.172 <u>+</u> .002	0.489 <u>+</u> .002
	0.784 <u>+</u> .003	-1.171 <u>+</u> .002	0.489 <u>+</u> .002
04	-1.040 <u>+</u> .002	0.000	-0.641 <u>+</u> .002
	-1.040 <u>+</u> .002	0.000	-0.641 <u>+</u> .002
c ₅	-1.909 <u>+</u> .002	0.000	0.516 <u>+</u> .002
	-1.909 <u>+</u> .002	0.000	0.516 <u>+</u> .002
H ₆	-2.949 <u>+</u> .002	0.000	0.190 <u>+</u> .002
	-2.934 <u>+</u> .002	0.000	0.146 <u>+</u> .002
H ₇	-1.716 <u>+</u> .002	0.889 <u>+</u> .002	1.115 <u>+</u> .002
	-1.742 <u>+</u> .002	0.889 <u>+</u> .002	1.123 <u>+</u> .002
Н ₈	-1.716 <u>+</u> .002	-0.889 <u>+</u> .002	1.115 <u>+</u> .002
	-1.742 <u>+</u> .002	-0.889 <u>+</u> .002	1.123 <u>+</u> .002

a Coordinates for tilted methyl are given in second line.

b In Angstroms.



Table 25. Calculated Bond Lengths^a and Bond Angles^b for Methoxydifluoro-phosphine.

	Symmetric	Methyl Group	
(PF)	1.587 <u>+</u> .005	<(FPF)	95.2 <u>+</u> .4
(PO)	1.569 <u>+</u> .006	<(FPO)	101.7 <u>+</u> .3
(OC)	1.446 <u>+</u> .006	<(POC)	123.5 <u>+</u> .4
(CH)	1.090 <u>+</u> .003	<(OCH)	109.5 <u>+</u> .2
		<(HCH)	109.4 <u>+</u> .2
	"Tilted"	Methyl Group	
(PF)	1.586 <u>+</u> .005	<(FPF)	95.3 <u>+</u> .4
PO)	1.572 <u>+</u> .006	<(FPO)	101.5 <u>+</u> .3
(OC)	1.446 <u>+</u> .006	<(POC)	123.5 <u>+</u> .4
(CH)	1.090 <u>+</u> .003	<(OCH ₆)	107.1 <u>+</u> 2
		<(0CH ₇)	110.7 <u>+</u> .2
		<(HCH)	109.4 + .2

a In Angstroms.

b In degrees.

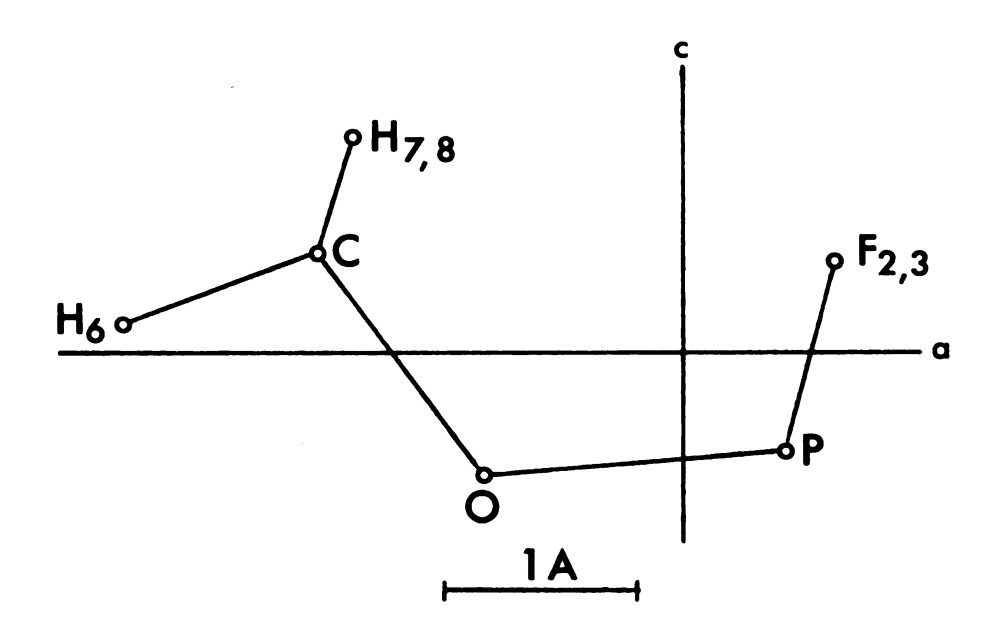


Figure VIII. Projection of methoxydifluorophosphine in the molecular plane of symmetry.

derivatives, has estimated the PO single and double bond lengths to be 1.71 and 1.38 Å, respectively. The shortening of the PO bonds given in Table 26, which should be single bonds, has been postulated as due to an increase in the PO bond order. In this respect, it would seem reasonable to conclude that the PO bond in this study, whose bond length agrees well those of Table 26, has also been shortened due to some form of multiple bonding.

The reported CO bond length in dimethyl ether (64) (1.417 Å) may be compared to that in methyl nitrate (63) (1.43 Å). The high barrier (9.1 kcal/mole) to the internal rotation of the nitrate group in methyl nitrate has suggested a partial double bond between the oxygen attached to the carbon and the nitrogen atom. Presumably such double bond character would result in a lengthening of the adjacent CO bond. Comparison of the CO bond length in this study, 1.446 Å, to that of methyl nitrate and those shown in Table 26 indicates that the CO bond length CH_3OPF_2 is longer than expected for a simple single bond, presumable a result of multiple bonding in the PO bond.

6.6 Discussion of Results

The most stable conformer of methoxydifluorophosphine apparently has a plane of symmetry with the methyl group cis to the fluorine atoms. This was not predicted since in this configuration there is an opportunity for steric hindrance between the hydrogens and the fluorine atoms. Indeed, two pieces of evidence from the final results suggest that some steric effects are operating. First, the barrier to internal rotation of the methyl group is low, even for a CH₃OX molecule (Table 18). If it is assumed that the equilibrium configuration of the methyl group occurs with the OP bond staggering the CH bonds, at equilibrium the two hydrogens

Table 26. Comparison of Results of Structural Studies on some Phosphorous (V) Compounds.

Molecule	Formula	d(P0)	q(0c)	<(P0C)	Ref.	
2,4,5-trimethoxy-1,3,5-trimethyl-						ı
2,5,6-trioxocyclotriphosphazane	_{N3} ме ₃ Р ₃ 0 ₃ (Оме) ₃	1.56 Å	1.45 Å	119°	89	
Methyl ethylene phosphate	C3H5PO4	1.57	1.44	118.8	69	82
Methyl diphenyl-thiophosphinite	C ₁₃ H ₁₃ SP0	1.60	1.45	118.5	70	
Methoxydifluorophosphine	CH ₃ 0PF ₂	1.572	1.446	123.5	this work	×ork

are near their point of closest approach to the fluorine atoms. A steric interaction in this configuration would tend to raise the minimum of the potential function, which would in turn reduce the barrier height. The second evidence for steric interaction is the result that the hydrogens of the methyl group appear to be tilted off the CO axis. The tilt is in the direction which moves the hydrogens away from the fluorines. For the proposed structure the minimum HF distance is $2.62 \, \text{Å}$ (the sum of van der Waals' radii is $2.55 \, \text{Å}$). Without the tilt the minimum HF distance would be $2.59 \, \text{Å}$.

The COP angle (123.5°) suggests the sp^2 hybrid orbitals are used by the oxygen atom to form the OC and OP bonds. The oxygen lone pairs could then be described by a p orbital perpendicular to the plane of symmetry and another sp^2 hybrid. The p orbital would have the correct symmetry for $(p \! + \! d)_{\pi}$ bonding with a phosphorus d orbital. As mentioned above, there is evidence that the PO bond is shorter than a hypothetical pure single bond. In this description, however, the sp^2 oxygen lone pair and the phosphorous lone pair should repel one another and lengthen the PO bond.

As discussed in the chapter on methyldifluorophosphine, results of recent studies of PF_2X derivatives suggest a dependence of the PF bond length on the electronegativity of the group X. Since the PF distance in CH_3OPF_2 is very nearly equal to that reported for PF_2NH_2 (Table 15), this suggests that the effective electronegativity of the $-NH_2$ and $-OCH_3$ groups are the same. In view of the similar inductive effects of these two substituents this result is not surprising.

LIST OF REFERENCES

LIST OF REFERENCES

- 1. C. E. Cleeton and N. H. Williams, Phys. Rev., 45, 234 (1934).
- 2. B. Bleaney and R. P. Penrose, Nature, 157, 339 (1946).
- 3. B. Bleaney and R. P. Penrose, Phys. Rev., 70, 775 (1946).
- 4. D. K. Coles and W. E. Good, Phys. Rev., 70, 979 (1946).
- 5. R. H. Hughes and E. B. Wilson, Jr., Phys. Rev., 71, 562 (1947).
- 6. T. W. Dakin, W. E. Good and D. K. Coles, Phys. Rev., 70, 560 (1946).
- 7. S. Golden and E. B. Wilson, Jr., J. Chem. Phys., 16, 669 (1948).
- 8. H. H. Nielsen, Phys. Rev., 40, 445 (1932).
- 9. J. S. Koehler and D. M. Dennison, Phys. Rev., 57, 1006 (1940).
- 10. R. W. Kilb, C. C. Lin, and E. B. Wilson, Jr., J. Chem. Phys., <u>26</u>, 1965 (1957).
- ll. D. R. Herschbach, J. Chem. Phys., <u>31</u>, 91 (1959).
- 12. E. B. Wilson, Jr., Adv. Chem. Phys., 2, 367 (1959).
- 13. J. Kraitchman, Am. J. Phys., <u>21</u>, 17 (1953).
- 14. C. C. Costain, J. Chem. Phys., <u>29</u>, 864 (1958).
- 15. H. H. Nielsen, Revs. of Mod. Phys., <u>23</u>, 90 (1951).
- 16. D. R. Herschbach and V. W. Laurie, J. Chem. Phys., <u>37</u>, 1668 (1962).
- 17. H. Goldstein, <u>Classical Mechanics</u>, Addison-Wesley Publishing Company, Inc., Reading, Massachusetts, 1950, p. 149.
- 18. H. C. Allen, Jr. and P. C. Cross, Molecular Vib-Rotors, John Wiley and Sons, Inc., New York, 1963, p. 5.
- 19. H. Erying, J. Walter and G. E. Kimble, Quantum Chemistry, John Wiley and Sons, Inc., New York, 1944, p. 39.
- 20. Reference 18, p. 10.

List of References (Continued)

- 21. J. Wollrab, <u>Rotational Spectra and Molecular Structure</u>, Academic Press, New York, 1967, p. 12.
- 22. G. W. King, R. M. Hainer and P. C. Cross, J. Chem. Phys., 11, 27 (1943).
- 23. Reference 21, p. 19.
- 24. S. C. Wang, Phys. Rev., 34, 243 (1929).
- 25. <u>Tables Relating to Mathieu Functions</u>, Columbia University Press, New York (1951).
- 26. R. W. Kilb, <u>Tables of Degenerate Mathieu Functions</u>, Harvard University Press, Cambridge, Massachusetts (1956).
- 27. B. L. Crawford, Jr., J. Chem. Phys., 8, 273 (1940).
- 28. D. R. Herschbach, <u>Tables for the Internal Rotation Problem</u>, Harvard University Press, <u>Cambridge</u>, <u>Massachusetts</u> (1957).
- 29. C. Olin and J. D. Swalen, Rev. Mod. Phys., 31, 84 (1959).
- 30. C. C. Lin and J. D. Swalen, Rev. Mod. Phys., 31, 841 (1959).
- 31. Reference 21, p. 244.
- 32. C. H. Townes and A. L. Schawlow, <u>Microwave Spectroscopy</u>, McGraw Hill Book Company, New York, 1955, p. 248.
- 33. R. H. Schwendeman, J. Mol. Spectry., 7, 280 (1961).
- 34. H. N. Volltrauer, Ph.D. Thesis, Michigan State University, 1970, Section 4.
- 35. R. S. Rogowski, Ph.D. Thesis, Michigan State University, 1968, Section 3.
- 36. Reference 21, Chapter 9.
- 37. Reference 32, Chapters 14-17.
- 38. H. N. Volltrauer and R. H. Schwendeman, J. Chem. Phys., 54, 260 (1971).
- 39. H. N. Volltrauer and R. H. Schwendeman, J. Chem. Phys., 54, 268 (1971).
- 40. P. L. Lee, Ph.D. Thesis, Michigan State University, 1971.
- 41. W. Lüttke and A. de Meijere, Angew. Chem. Internal. Edit., <u>5</u>, 512 (1966).
- 42. A. de Meijere and W. Lüttke, Tetrahedron 25, 2047 (1969).

List of References (Continued)

- 43. J. H. Hand, Ph.D. Thesis, Michigan State University, 1965.
- 44. M. W. P. Strandberg, <u>Microwave Spectroscopy</u>, John Wiley and Sons, Inc., New York, 1954, p. 4.
- 45. Reference 34, Chapter V.
- 46. D. R. Lide, Jr. and D. E. Mann, J. Chem. Phys., 27, 868 (1957).
- 47. V. W. Laurie, J. Chem. Phys., 34, 1516 (1961).
- 48. D. R. Lide, Jr. and D. E. Mann, Ibid., 864 (1957).
- 49. D. R. Lide, Jr. and M. Jen, J. Chem. Phys., 40, 252 (1964).
- 50. A. H. Brittain, J. E. Smith, P. L. Lee, K. Cohn and R. H. Schwendeman, to be published.
- 51. A. H. Brittain, J. E. Smith and R. H. Schwendeman, to be published.
- 52. P. L. Lee, Ph.D. Thesis, Michigan State University, 1971, Section 6.
- 53. This Thesis, Section 6.
- 54. R. L. Kuczkowski, J. Am. Chem. Soc., 90, 1705 (1968).
- 55. T. Kojima, E. L. Breig and C. C. Lin, J. Chem. Phys., <u>35</u>, 2139 (1961).
- 56. K. Shimoda, T. Nishikawa and T. Itoh, Phys. Rev., 98, 1160 (1955).
- 57. L. Pierce, R. G. Hayes and J. F. Beecher, J. Chem. Phys., 46, 4353 (1967).
- 58. L. J. Nugent and C. D. Cornwall, J. Chem. Phys., 37, 523 (1962).
- 59. Reference 21, p. 30.
- 60. Rotational Energy Levels of Asymmetric Top Molecules, Tables of Reduced Energies, Grumman Research Department, Grumman Aircraft Engineering Corporation, Bethpage, New York.
- 61. E. V. Ivash and D. M. Dennison, J. Chem. Phys., 21, 1804 (1953).
- 62. R. F. Curl, Jr., J. Chem. Phys., 30, 1529 (1959).
- 63. W. B. Dixon and E. B. Wilson, Jr., J. Chem. Phys., 35, 191 (1961).
- 64. P. H. Kasai and R. J. Meyers, J. Chem. Phys., 30, 1099 (1959).
- 65. D. R. Herschbach, <u>Bibliography for Hindered Internal Rotation and Microwave Spectroscopy</u>, Lawrence Radiation Laboratory, Berkeley, California, UCRL-10404 (1963).

List of References (Continued)

- 66. V. W. Laurie and D. R. Herschbach, J. Chem. Phys., 37, 1687 (1962).
- 67. Reference 35, Section 6.
- 68. G. B. Ansell and G. J. Bullen, J. Chem. Soc. (A), 3026 (1968).
- 69. T. A. Steitz and W. N. Lipscomb, J. Amer. Chem. Soc., <u>87</u>, 2488 (1965).
- 70. P. G. Lepicard, D. De-Saint-Giniez-Liebig, A. Laurent and C. Rerat, Acta. Cryst., <u>25B</u>, 617 (1969).
- 71. D. W. J. Cruickshank, J. Chem. Soc., 5486 (1961).
- 72. H. V. Malmstadt and C. G. Enke, <u>Digital Electronics for Scientists</u>, W. A. Benjamin, Inc., New York, 1969, Chapter 4.

APPENDIX

A binary decoder was designed to provide a convenient and accurate method of placing frequency markers directly on a spectral recording. To accomplish this it was necessary to distinguish between the various binary representations of one digit of the microwave frequency as supplied by a Hewlett-Packard 5245 L counter fitted with a Hewlett-Packard 5257 A transfer oscillator. The binary representations of the decimal numbers zero to nine are given in Table 27. A combination of integrated circuit solid state devices called NAND gates, AND gates and OR gates was used to differentiate between the various representations. The symbols and truth tables for these devices are given in Figure IX, (72). The states O and I may be conveniently represented electronically by voltages of O and +5 volts respectively; this representation may be extended to the binary representation given in Table 27. When all the inputs of a NAND gate are in state 1 (at +5 volts) the output will be in state 0 (at 0 volts). This is the unique situation, since the output will be in state 1 for all other input combinations. For an AND gate the unique output is state 1 and occurs when all inputs are in state 1. For an OR gate the unique output is state 0 and occurs when all inputs are in state 0.

An example of a combination of gates which may be used to differentiate between zero and the other representations of Table 27 is shown below:

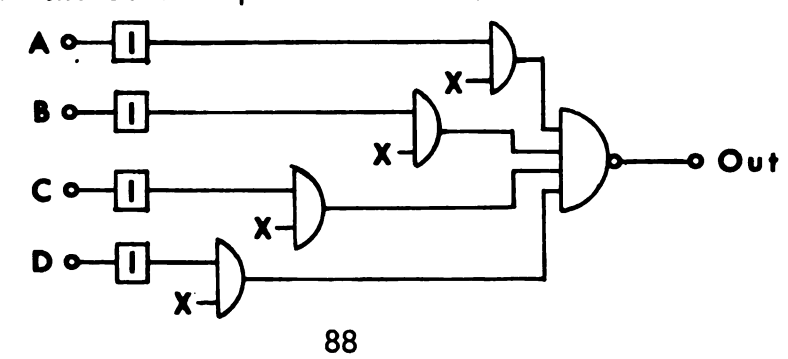


Table 27. Binary Representation of the Decimal Numbers Zero to Nine.

	20	21	2 ²	2 ³
0	0	0	0	0
1	1	0	0	0
2	0	1	0	0
3	1	1	0	0
4	0	0	1	0
5	1	0	1	0
6	0	1	1	0
7	1	1	1	0
8	0	0	0	. 1
9	1	0	0	1

,	A OF D	Out		Ao- Bo-	-o Out	,	40	≻ -•Out
<u>A</u>	В	Out	<u>A</u>	В	Out	<u>A</u>	В	Out
0	0	1	0	0	0	0	0	0
1	0	1	1	0	0	1	0	1
0	1	1	0	1	0	0	1	1
1	1	0	1	1	1	1	1	1
	(a)			(b))		(c)	

Figure IX. Symbols and truth tables for (a) NAND gates, (b) AND gates and (c) OR gates.

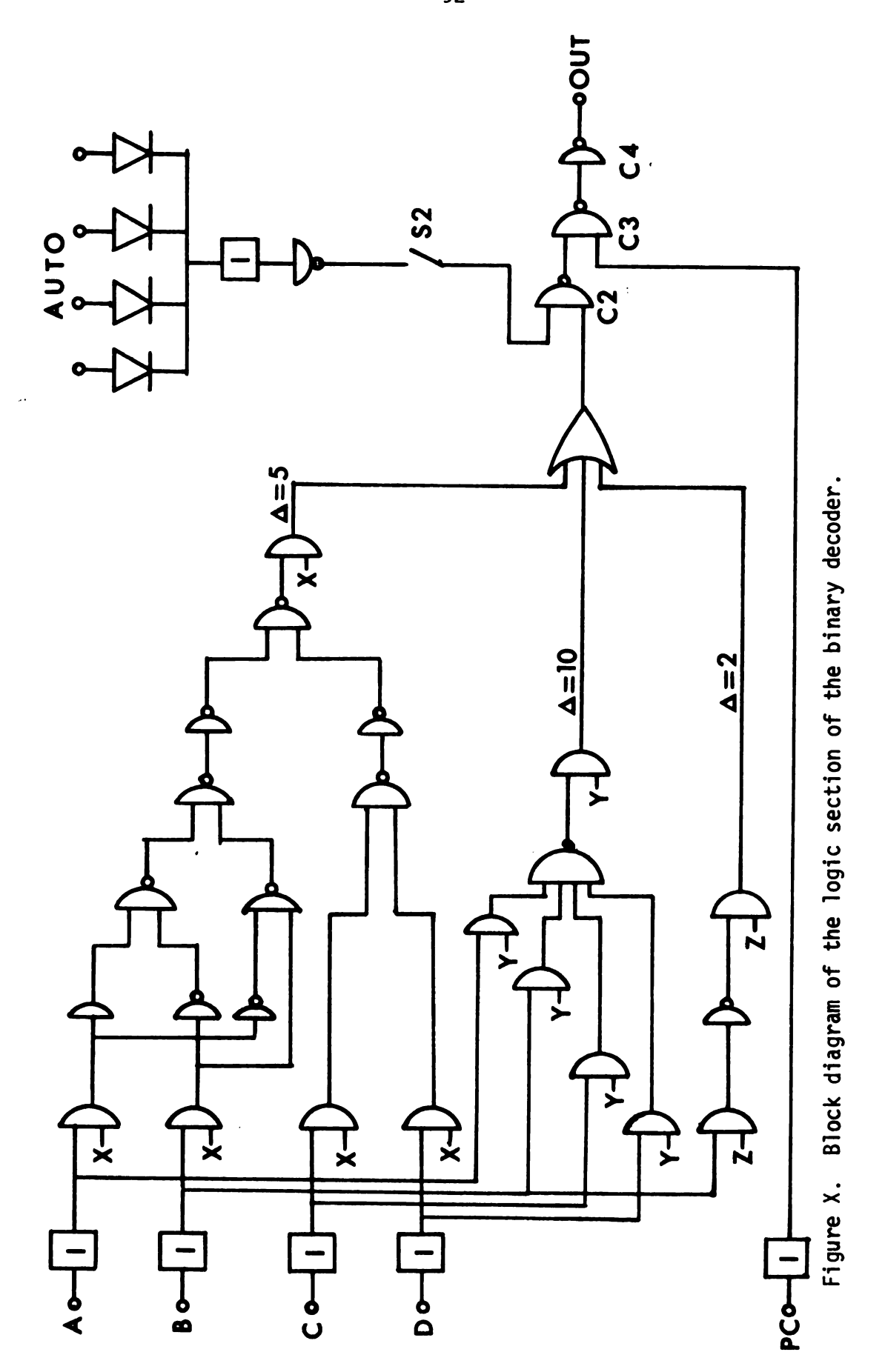
The circuitry represented by "I" is designed to insure that the incoming signal has the proper voltage (0 volts for state 0 and \pm 5 volts for state 1) and to invert the input state (0 \pm 1 and 1 \pm 0). The X inputs to the AND gates are held in state 1. Thus, if all the binary inputs are zero, they are inverted to ones by the I circuits and mixed with ones from the X's. From Figure IXb it is seen that the outputs of the AND gates will be all ones. Any other decimal input will have at least one binary input non-zero, and hence at least one AND gate output equal to zero. If all the AND gate outputs are one, the NAND gate output will be zero (Figure IXa). If any one (or more) of the AND gate outputs is zero, the NAND gate output will be one. In this manner the decimal digit zero may be distinguished from the other decimal digits. The output state 0 (0 volts) may be manipulated in any convenient manner to activate the events marker pen and place a frequency marker on the recording.

横口を はなければ 日本には おおからからなる かっている ののない ないしゅん

Since frequency markers were desired in intervals of 2, 5 or 10 units (the magnitude of the intervals depends upon which digit is being monitored), the decoder consists of three sections, one for each interval. The logic diagram of the decoder is given in Figure X, where the three sections of the decoder are identified according to the resulting marker intervals.

Switching from one logic section to another, i.e. from one marker interval to another, is accomplished by means of the X, Y and Z inputs to the AND gates. When these inputs are in state 0 the output must be state 0 and the section is "turned off". In the previous example X was in state 1 while Y and Z were in state 0.

The inputs A, B, C and D may be mechanically switched to monitor any one of the four right-most digits of the counter's display. For normal counting rates the decimal point of the displayed frequency is two digits from the right; thus, digits representing 10 kHz to 10 MHz may be monitored.



The PC input in Figure X is a print command from the counter which indicates when the counting cycle has been completed and the measured frequency is ready to be monitored. While the counter is "counting" PC is in state 1. When the cycle is complete, PC switches to state 0 which is inverted to state 1 and locks the output of C3 to either state 0 or 1 depending upon whether the other input is 0 or 1, respectively. In the previous example the unique output was 0 which would pass the OR gate as 0 and be inverted by C2 to state 1. If PC is in state 0 both inputs to C3 will be in state 1 resulting in an output state 0 which is inverted by C4 to state 1 which represents the unique output state of the decoder.

Closing S2 introduces the "auto" section into the circuit. This section may be mechanically switched to monitor any one of the second through fifth digits from the right of the counter. In normal operation S2 is switched to the digit just to the left of the one being monitored by inputs A, B, C and D. The purpose of this section is to provide continuous markers whenever the digit being monitored is zero, regardless of the situation existing at inputs A, B, C and D. For example, if markers are being placed on the recording in 5 MHz intervals then every twentieth marker, i.e., every 100 MHz, will be broader then the others. This function is very useful in correlating the markers with the correct frequencies.

